





# Amniotic membrane-mesenchymal stromal cells secreted factors and extracellular vesicle-miRNAs: Anti-inflammatory and regenerative features for musculoskeletal tissues

Enrico Ragni<sup>1</sup>  | Andrea Papait<sup>2,3</sup> | Carlotta Perucca Orfei<sup>1</sup>  |  
 Antonietta Rosa Silini<sup>2</sup>  | Alessandra Colombini<sup>1</sup> | Marco Viganò<sup>1</sup>  |  
 Francesca Libonati<sup>1</sup> | Ornella Parolini<sup>3,4</sup> | Laura de Girolamo<sup>1</sup>

<sup>1</sup>IRCCS Istituto Ortopedico Galeazzi, Laboratorio di Biotecnologie Applicate all'Ortopedia, Milan, Italy

<sup>2</sup>Centro di Ricerca E. Menni, Fondazione Poliambulanza Istituto Ospedaliero, Brescia, Italy

<sup>3</sup>Department of Life Science and Public Health, Università Cattolica del Sacro Cuore, Rome, Italy

<sup>4</sup>Fondazione Policlinico Universitario "Agostino Gemelli" IRCCS, Rome, Italy

## Correspondence

Laura de Girolamo, PhD, IRCCS Istituto Ortopedico Galeazzi, Laboratorio di Biotecnologie Applicate all'Ortopedia, Via R. Galeazzi 4, I-20161 Milan, Italy.  
Email: laura.degirolamo@grupposandonato.it

## Funding information

PRIN 2017 program of Italian Ministry of Research and University (MIUR), Grant/Award Number: 2017RSAFK7 to Ornella Parolini; Intramural funds from the Università Cattolica del Sacro Cuore, Grant/Award Numbers: Linea D1-2019, Linea D1-2018; Italian Ministry of Health, MIUR (5x1000 year 2017); Fondazione Poliambulanza of Brescia; Italian Ministry of Health, "Ricerca Corrente"

## Abstract

Human amniotic membrane-derived mesenchymal stromal cells (hAMSCs) are easily obtained in large quantities and free from ethical concerns. Promising therapeutic results for both hAMSCs and their secreted factors (secretome) were described by several in vitro and preclinical studies, often for treatment of orthopedic disorders such as osteoarthritis (OA) and tendinopathy. For clinical translation of the hAMSC secretome as cell-free therapy, a detailed characterization of hAMSC-secreted factors is mandatory. Herein, we tested the presence of 200 secreted factors and 754 miRNAs in extracellular vesicles (EVs). Thirty-seven cytokines/chemokines were identified at varying abundance, some of which involved in both chemotaxis and homeostasis of inflammatory cells and in positive remodeling of extracellular matrix, often damaged in tendinopathy and OA. We also found 336 EV-miRNAs, 51 of which accounted for more than 95% of the genetic message. A focused analysis based on miRNAs related to OA and tendinopathy showed that most abundant EV-miRNAs are teno- and chondro-protective, able to induce M2 macrophage polarization, inhibit inflammatory T cells, and promote Treg. Functional analysis on IL-1 $\beta$  treated tenocytes and chondrocytes resulted in downregulation of inflammation-associated genes. Overall, presence of key regulatory molecules and miRNAs explain the promising therapeutic results of hAMSCs and their secretome for treatment of musculoskeletal conditions and are a groundwork for similar studies in other pathologies. Furthermore, identified molecules will pave the way for future studies aimed at more

Enrico Ragni and Andrea Papait contributed equally to the work.

This is an open access article under the terms of the Creative Commons Attribution-NonCommercial-NoDerivs License, which permits use and distribution in any medium, provided the original work is properly cited, the use is non-commercial and no modifications or adaptations are made.

© 2021 The Authors. STEM CELLS TRANSLATIONAL MEDICINE published by Wiley Periodicals LLC on behalf of AlphaMed Press.

sharply predicting disease-targeted clinical efficacy, as well as setting up potency and release assays to fingerprint clinical-grade batches of whole secretome or purified components.

**KEYWORDS**

amnion, extracellular vesicles, inflammation, mesenchymal stem/stromal cells, osteoarthritis, tendinopathy

## 1 | INTRODUCTION

Mesenchymal stromal cells (MSCs) gained privileged attention in the field of regenerative medicine due to their combined anti-inflammatory and tissue progenitor activating features.<sup>1</sup> At present (October 2020), over 1100 registered clinical trials investigating the use of MSCs are registered (<https://clinicaltrials.gov/>), among which most are related to musculoskeletal and immunological conditions.<sup>2</sup>

The most common MSCs sources are currently bone marrow and adipose tissue,<sup>3</sup> although ethical and safety concerns led to the search for alternatives. Conversely, the amniotic membrane is an advantageous MSC source, since placenta is normally discarded after birth and its collection and use free from ethical controversy.

Human amniotic membrane-derived MSCs (hAMSCs) possess strong immunomodulatory properties promoting tissue repair and regeneration through paracrine mechanisms.<sup>4</sup> hAMSCs suppress the *in vitro* proliferation, inflammatory cytokine production, and functions of T lymphocytes, monocytes, dendritic cells, macrophages, and natural killer cells.<sup>4-6</sup> In addition, hAMSCs induce M2 macrophages with anti-inflammatory, pro-regenerative characteristics and support the expansion of regulatory T cells.<sup>4,7,8</sup> Furthermore, both hAMSCs and the amniotic membrane have shown promising outcomes in orthopedic applications. In an *in vitro* osteoarthritis (OA) model, hAMSCs improved chondrocyte viability and enhanced the anti-inflammatory M2-phenotype switch,<sup>9</sup> while *in vivo* hAMSCs stimulated the repair of cartilage defects and inhibited T-cell response.<sup>10</sup> In humans, hAMSCs-enriched amniotic suspension allografts (ASAs) improved pain and functional scales of patients with symptomatic knee OA.<sup>11</sup> Similar results were obtained in tendinopathies treatment, where ASA and amniotic membrane fragments improved fiber alignment and restored a physiological-like cell density in rats.<sup>12,13</sup> Due to the above reasons, hAMSCs are being explored in both immune-related (NCT02172924, NCT01769755) and orthopedic (NCT03337243, NCT03028428) clinical trials.

Nevertheless, hAMSCs functional and molecular characterization remains fragmentary, delaying their wider translation in clinical practice. It has been proposed that MSCs mode of action is mediated by secreted cytokines and growth factors,<sup>14</sup> as well as different types of extracellular vesicles (EVs),<sup>15</sup> altogether defined as the secretome. Consistently, hAMSC-secreted factors have been shown to induce antiproliferative effects on T cells, skew their polarization to favor T regulatory cells (Treg), inhibit the differentiation of monocyte-derived dendritic cells,<sup>16,17</sup> and decrease pro-inflammatory M1

### Significance statement

The therapeutic potential of human amniotic membrane-derived mesenchymal stromal cells (hAMSCs) has been addressed to both soluble factors and extracellular vesicles (EVs). This study characterized the abundance of 200 factors and 754 EV-miRNAs released by hAMSCs. Identified molecules share protective signals in those contexts where inflammation and degeneration have to be counteracted, such as osteoarthritic joints or pathological tendons, and support preliminary *in vitro* and preclinical studies. These data allow for prediction of a broader disease-targeted clinical efficacy, as well as the setup of potency and release assays to fingerprint clinical-grade batches of hAMSCs cell-free products.

differentiation and activation thus promoting M2 macrophage polarization<sup>7,8</sup> and activation.<sup>18</sup> The hAMSC secretome was also able to induce collagen production and biomechanical properties at the site of Achilles tendon transection in rats.<sup>19</sup> Similarly, in patients with tendinosis, injection of amnion/chorion membrane allograft containing hAMSCs-secreted factors led to pain reduction and functional improvement,<sup>20</sup> consistent with what was also observed in a rabbit model with osteochondral defects.<sup>21</sup> Furthermore, in equine models, purified hAMSC-derived EVs were demonstrated to act as key players in tendon lesion healing and to exert an anti-inflammatory effects on tenocytes, and these effects were largely mediated by EV-embedded miRNAs.<sup>22,23</sup> Taken together, these results strongly support the therapeutic actions of hAMSC-released factors.

A wide screening of soluble molecules, either free or EV-conveyed, is therefore crucial and mandatory to predict a disease-targeted clinical potency. Also, identification of reliable markers may define future release assays to frame the fingerprint of clinical-grade batches of hAMSCs secretome or purified components, such as EVs, in order to use naïve or engineered cell-free clinical products with increased potency. In this work, 200 soluble factors and 754 miRNAs were quantified in the hAMSC secretome and in purified EVs, respectively. Findings of the study have been critically discussed in the frame of OA and tendinopathy to give ground to the encouraging observations reported by both *in vitro* and preclinical studies since, although sharing few etiopathogenetic factors, both conditions are often treated with similar approaches, including the use of cell therapy products.

## 2 | MATERIALS AND METHODS

### 2.1 | hAMSCs isolation, expansion, and secretome production

Human term placentas ( $n = 3$ ) were collected from healthy women and processed. hAMSCs were isolated as previously described,<sup>24</sup> and cultured in complete CHANG C Medium at 37°C, 5% CO<sub>2</sub>, and 95% humidity until passage 2 and 3, before secretome production and flow cytometry analysis. Complete CHANG C medium was obtained by adding lyophilized supplements to basal CHANG B medium (Irvine Scientific, Irvine, California; see [http://www.irvinesci.com/uploads/technical-documentations/40200\\_Chang\\_C\\_T101\\_C100\\_Rev12.pdf](http://www.irvinesci.com/uploads/technical-documentations/40200_Chang_C_T101_C100_Rev12.pdf)), to obtain a final concentration of 6% newborn calf serum and 6% fetal bovine serum (<http://www.irvinesci.com/chang-media-faq>). For secretome production, hAMSCs at 90% confluency were washed three times with Phosphate Buffered Saline (PBS) to remove protein supplements contamination, and 12 mL of serum-free and supplement-free CHANG B medium was added per T175 cell culture flask. Secretome was collected after 48 hours and serially centrifuged (376g, 1000g, 2000g, and twice at 4000g, 15 minutes each) at 4°C to eliminate debris, floating cells and apoptotic bodies. Cleared secretome was directly used for enzyme-linked immunosorbent assay (ELISA) analysis or further processed for EVs isolation.

### 2.2 | hAMSCs characterization

Flow cytometry was performed with CytoFlex (Beckman Coulter, Fullerton, California) flow cytometer (minimum 30 000 events), with CD90-FITC (REA897), CD73-PE (REA804), CD34-FITC (AC136), CD45-PEVIO770 (REA747) and CD31-PERCPVIO700 (REA730) (Miltenyi, Bergisch Gladbach, Germany), and CD44-PERCP (44PP2) (Immunostep, Salamanca, Spain) antibodies.<sup>25</sup>

### 2.3 | ELISA assays

The concentration of 200 soluble cytokines, receptors, chemokines, growth, and inflammatory factors (Table S1) was determined by Quantibody Human Cytokine Array 4000, according to manufacturers' instructions (RayBiotech, Norcross, Georgia). Only factors with positive detection above single assays threshold in all samples were selected. The amount per cell (ng/10<sup>6</sup> cells) was obtained by multiplying the concentration in ng/mL per total volume and dividing per million cells.

### 2.4 | Secretome protein-protein interaction networks

Interactome maps were constructed by STRING (<http://www.string-db.org>) (database v11 data accessed: July 2020). Network properties were selected as follows: organism, *Homo sapiens*; meaning of network edges, evidence; active interaction sources, experiments and

databases; minimum required interaction scores, medium confidence (0.400).

### 2.5 | Identification of enriched gene ontology terms

GORilla tool (<http://cbl-gorilla.cs.technion.ac.il/>) was used sifting two unranked lists, either ELISA or STRING 1/2 clusters and the 200 molecules of the ELISA array, as targets and the background, respectively.<sup>26</sup>  $P$  value threshold  $<10^{-3}$ .

### 2.6 | EVs isolation and characterization

EVs were obtained by centrifuging cleared secretome (100 000g, 9 hours, 4°C) in a 70Ti rotor (Beckman Coulter). One hundred microliters of PBS per initial 10 mL was used to suspend EV pellets and processed as follows:

- Flow cytometry: After a 1:150 dilution in PBS, carboxyfluorescein succinimidyl ester (CFSE) was added at a final concentration of 100 nM and left to incubate for 30 minutes at 37°C. The following antibodies (all from Biolegend, San Diego, California) were individually added to labeled EVs following manufacturers' instructions: CD9-APC (HI9A), CD63-APC (H5C6), and CD81-APC (5A6) for EV<sup>27</sup> or CD44-APC (BJ18), CD73-APC (AD2), and CD90-APC (5E10) as MSC markers.<sup>28</sup> After a subsequent 1:7 dilution in PBS, samples were analyzed with a CytoFlex flow cytometer (minimum 30 000 events) and compared with 160-200-240-500 nm fluorescein isothiocyanate (FITC)-fluorescent beads (Biotex, Marseille, France). PBS supplemented with CFSE and unstained EVs were used as background controls.
- Transmission electron microscopy: 5  $\mu$ L EVs were absorbed on Formvar carbon-coated grids. Negative stain was performed with 2% uranyl acetate (10 minutes). Excess was removed by filter paper before drying the grid at room temperature (RT). Samples were examined with a TALOS L120C transmission electron microscope (Thermo Fisher Scientific, Waltham, Massachusetts) at 120 kV.
- Nanoparticle tracking analysis (NTA): EVs were diluted 1:500 in PBS and visualized by Nanosight LM10-HS system (NanoSight Ltd., Amesbury, UK). Five recordings (60 seconds) were performed. NTA software provided high-resolution particle size distribution profiles and concentration measurements. The same procedure was followed for the analysis of the cleared secretome diluted 1:5 in PBS. Dilution factors were used to calculate particle concentration.

### 2.7 | Amplification of EV-embedded miRNAs by quantitative real time-polymerase chain reaction (qRT-PCR)

Trizol reagent was used to dissolve EV pellets. RNA was extracted with miRNeasy and RNeasy CleanUp Kits following manufacturer's

instructions (Qiagen, Hilden, Germany). Six picograms of a non-human synthetic miRNA (*Arabidopsis thaliana* ath-miR-159a) were added as a spike-in before RNA extraction in order to monitor technical variability during isolation and during subsequent reactions for the eventual equalization of panels A and B of the OpenArray platform (Life Technologies). Standard reverse transcription and preamplification procedures with A and B independent kits were followed for cDNAs synthesis. As previously described,<sup>29</sup> real-time RT-PCR analysis with the QuantStudio 12 K Flex OpenArray Platform (QS12KFlex) was performed on A and B miRNA panels, that together cover 754 human miRNA sequences from the Sanger miRBase v21.  $C_{RT} \geq 28$  were considered as unamplified reactions. After equalization of A and B plates for each sample by ath-miR-159a  $C_{RT}$  values, the global mean normalization was used.<sup>30</sup>  $C_{RT}$  values for each amplified miRNA were reported.

## 2.8 | EV-miRNAs hierarchical clustering

ClustVis package (<https://biit.cs.ut.ee/clustvis/>) was used to generate heat map plots for EV-miRNAs using normalized  $C_{RT}$  values for each sample. Clustering options were: distance for rows-correlation, method for rows-average, and tree ordering for rows-tightest cluster first.

## 2.9 | EV-miRNAs target identification and functional analysis

miRNA targets were annotated with DIANA-miRPath v.3 (<http://snf-515788.vm.okeanos.grnet.gr/>), using microT-CDS to score for predicted miRNA-mRNA interactions (threshold 0.8) in CDS or 3'-UTR. For a more stringent analysis, an heat map of significant ( $P < .05$ ) miRNA signatures in the biological process gene ontology (GO) database was generated with the miRPath DB v2.0 heat map calculator ([https://mpd.bioinf.uni-sb.de/heatmap\\_calculator.html?organism=hsa](https://mpd.bioinf.uni-sb.de/heatmap_calculator.html?organism=hsa)) (database-Gene Ontology Biological Processes, evidence-experimental [strong], minimum number of significant miRNAs a pathway should have to be shown-1 or 10), using only experimentally validated miRNA-mRNA interactions. Experimentally strong miRNA-mRNA interactions shared by miR-24-3p and miR-146a-5p were eventually submitted to PANTHER web interface (<http://www.pantherdb.org/>) to identify proteins encompassing the same functional classifications, under v15.0 database and following settings: more than 50% of submitted proteins to display a functional category and "GO Biological Process complete" annotated data set (GO Ontology database released on March 23, 2020). False discovery rate calculation and  $P$  value  $< .05$  with Fisher's exact test type were also selected.

## 2.10 | Functional test

Chondrocytes were obtained from three OA (Kellgren Lawrence III or IV) patients undergoing total hip arthroplasty by harvesting cartilage with a scalpel from nonweight bearing superficial areas of femoral

head/neck. Chondrocytes were isolated by enzymatic digestion with 0.15 wt%/vol% type II collagenase (Worthington Biochemical, Lakewood, New Jersey). Tenocytes were obtained from discarded fragments of the semitendinosus and gracilis tendons harvested from three patients who underwent elective anterior cruciate ligament reconstruction using hamstring tendons. Tenocytes were isolated by enzymatic digestion with 0.3 wt%/vol% type I collagenase (Worthington Biochemical). Both chondrocytes and tenocytes were cultured in Dulbecco's modified Eagle medium (DMEM) + 10% phosphate buffered saline (FBS) and expanded until use. At passage 3 and 90% confluence, both cell types were cultured for 48 hours in CHANG C medium, CHANG C medium supplemented with 1 ng/mL IL-1 $\beta$  or hAMSC secretome (generated in CHANG B medium) supplemented with 1 ng/mL IL-1 $\beta$  and related supplements to obtain the complete "C" formulation. The medium/cells ratio was set to 5 mL per 250 000 cells in 25 cm<sup>2</sup> flasks. After treatment, cells were collected and frozen at  $-80^{\circ}\text{C}$  until RNA extraction.

RNA was extracted using RNeasy Plus Mini Kit (Qiagen, Frederick, Maryland). cDNA synthesis was performed using iScript cDNA Synthesis Kit (Biorad, Hercules, California). qRT-PCR was performed using iTaq Universal SYBR Green Supermix (Biorad) reagent and transcript-specific primers (*COL1/2/3*, *MMP1/13*, *CXCL8*, *TGFB*, *COX2*, *IL6*; sequences available on request), following the manufacturer's instructions. For each sample, independent qRT-PCR reactions in technical duplicate were performed using a StepOnePlus real-time PCR system thermocycler (Applied Biosystems, Thermo Fisher Scientific). *TBP* and *ACTB* were used as housekeeping genes for chondrocytes and tenocytes, respectively, to score transcript modulation across samples with the  $\Delta\Delta\text{Ct}$  (cycle threshold) method.

## 2.11 | Statistical analyses

Only EV-miRNAs or factors detected in all samples were considered. GraphPad Prism software (GraphPad, San Diego, California) was used for statistical analysis. The level of significance for the different tests was set to a minimum  $P$  value of  $< .05$  or  $< 10^{-3}$ , depending on analyses and algorithms' parameters.

# 3 | RESULTS

## 3.1 | hAMSCs and EVs phenotypic characterization

CD73, CD90, and CD44 MSC cell-surface antigens were highly expressed in hAMSCs, whereas hemato-endothelial markers CD31, CD34, and CD45 were not expressed (Figure 1A).

EV batches had an average protein concentration of  $0.08 \pm 0.01 \mu\text{g}/\mu\text{L}$  and  $2.62 \times 10^9 \pm 0.33$  particles/ $\mu\text{g}$  total protein, therefore depleted of major contaminants, such as protein aggregates or lipoproteins, that may affect size distribution profiling.<sup>31</sup> As assessed by NTA, EVs in both secretome and after isolation shared a superimposable dimensional profile, confirming that ultracentrifugation does

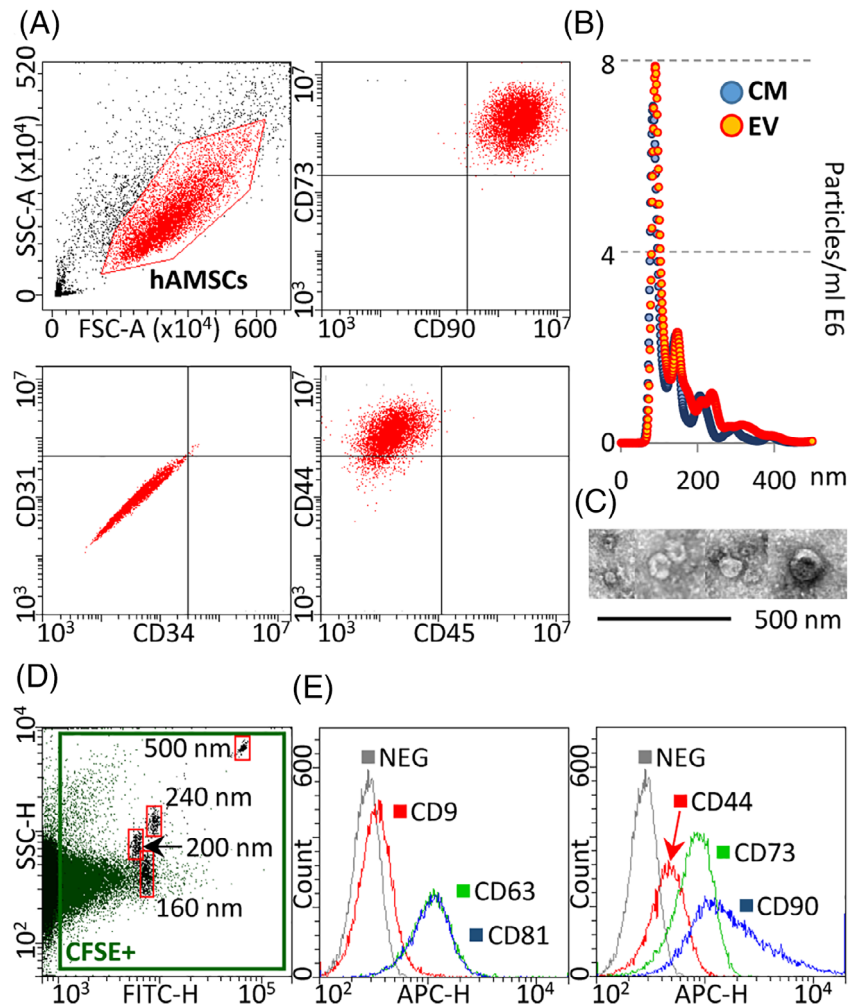


**FIGURE 1** hAMSCs and hAMSC-EVs phenotype characterization. A, Flow cytometry analysis of MSC staining (positive for CD44, CD73, and CD90; negative for hemato-endothelial markers CD31, CD34, and CD45), confirming hAMSCs identity. Representative plots are shown. B, EVs size distribution by NanoSight particle tracking analysis in both CM (blue dots) and purified EVs (orange dots). A representative plot from the same hAMSC donor is shown. C, Transmission electron micrographs of EVs showing particles with characteristic cup-shaped morphology. D, The resolution of the FITC-fluorescent reference bead mix indicates the flow cytometer performance in light scattering at default settings. The cytogram depicts the SSC-H vs 535/35 (green fluorescence triggering) channel, with four fluorescent nanobead populations (160, 200, 240, and 500 nm) compared with CFSE-stained EVs (in green the positive events), allowing their identification and gating in the FITC channel (CFSE+ gate) vs background noise, debris, and unstained particles. E, After CFSE+ gating, with respect to Ab-unstained samples (in gray), Ab-treated EVs showed the presence of extracellular vesicle defining molecules CD63 and CD81, while CD9 staining gave a weak signal. EVs were also strongly positive for MSC markers CD73 and C90. CD44 labeling allowed a complete peak shift of the population from the Ab-unstained sample, although without a sharp separation. Representative cytograms are presented. CFSE, carboxyfluorescein succinimidyl ester; CM, conditioned medium; EVs, extracellular vesicles; FITC, fluorescein isothiocyanate; hAMSCs, human amniotic membrane-derived mesenchymal stromal cells; MSC, mesenchymal stromal cell

not affect vesicle integrity or allow selection of a subpopulation (Figure 1B). EVs were within expected dimensional range (mode of  $84.1 \pm 1$  nm and  $89 \pm 1.4$  nm for conditioned medium (CM) and after purification, respectively). In purified EVs, >75% resulted below 200 nm with a D50 of  $122.4 \pm 4$  nm, thus enriched in small vesicles/exosomes. Absence of particles larger than 500 nm indicated efficient apoptotic bodies and cell debris removal. Transmission electron microscopy (TEM) supported NTA dimensional range (Figure 1C). Furthermore, CFSE staining confirmed vesicle integrity after ultracentrifugation and, by comparison with FITC-nanobeads (160-200-240-500 nm), size-range data were again validated

(Figure 1D). MSC-EV defining markers such as CD44, CD73 and CD90, and other generic EV-markers such as CD63 and CD81 were detected (Figure 1E). CD9 resulted weakly expressed on the entire population (Figure 1E), similar to other adult and foetal MSC-EVs.<sup>29,32</sup>

### 3.2 | hAMSCs secreted factors

The average protein concentration for the entire secretome was  $0.32 \pm 0.02$  mg/mL. Thirty-seven molecules were detected in all donors (Table 1). Correlation analysis showed a strong similarity ( $R^2 = 0.99$  for

donor 1 vs 2,  $R^2 = 0.97$  for 1 vs 3, and  $R^2 = 0.99$  for 2 vs 3), thus an average intensity value for each molecule was reported. Considering 1 million cells, only IGFBP4 was secreted with an amount higher than 100 ng ( $465 \pm 57$ ). Six molecules were between 100 and 10 ng (IGFBP6,  $92 \pm 6$ ; IGFBP3,  $55 \pm 29$ ; TIMP2,  $50 \pm 9$ ; SERPINE1,  $19 \pm 3$ ;

INHBA,  $16 \pm 25$ ; IL6,  $15 \pm 2$ ). Sixteen factors were between 10 and 1 ng and 14 molecules resulted below 1 ng.

Regardless the expression level, a functional protein association network analysis based on both experimental and database annotated interactions identified two clusters. The first cluster was tighter and

**TABLE 1** hAMSCs secreted factors

Type	Name	pg/10 <sup>6</sup> hAMSCs		Description
		Mean	SD	
GF	IGFBP4	464 609	56 058	Insulin-like growth factor-binding protein 4
GF	IGFBP6	92 274	6033	Insulin-like growth factor-binding protein 6
GF	IGFBP3	55 434	28 505	Insulin-like growth factor-binding protein 3
INF	TIMP2	50 298	8553	Metalloproteinase inhibitor 2
CYTO	SERPINE1	19 296	3351	Plasminogen activator inhibitor 1 (Serpine E1)
CYTO	INHBA	15 738	25 298	Inhibin beta A chain
INF	IL6	14 667	1578	Interleukin-6
CHE	SPP1	8847	3153	Osteopontin
INF	TIMP1	7095	673	Metalloproteinase inhibitor 1
GF	GDF15	5716	449	Growth/differentiation factor 15
REC	PLAUR	5707	967	Urokinase plasminogen activator surface receptor
REC	CD14	3389	1484	Monocyte differentiation antigen CD14
INF	ICAM1	2894	1830	Intercellular adhesion molecule 1
INF	TNFRSF1A	2850	1376	Tumor necrosis factor receptor superfamily member 1A
INF	CCL2	2754	581	C-C motif chemokine 2
REC	TNFRSF21	2408	2873	Tumor necrosis factor receptor superfamily member 21
GF	VEGFA	2394	1770	Vascular endothelial growth factor A
CHE	CXCL5	2180	539	C-X-C motif chemokine 5
CYTO	TGFB1	2103	258	Human TGF-beta 1
INF	CCL5	1975	566	C-C motif chemokine 5
CYTO	ANG	1950	434	Angiogenin
CHE	MIF	1840	1030	Macrophage migration inhibitory factor
CYTO	DKK1	1740	1124	Dickkopf-related protein 1
CHE	CXCL1	772	207	Growth-regulated alpha protein (C-X-C motif chemokine 1)
CHE	XCL1	597	318	Lymphotoxin (XC chemokine ligand 1)
INF	IL11	502	254	Interleukin-11
CHE	CXCL6	459	150	C-X-C motif chemokine 6
INF	CCL4	431	116	C-C motif chemokine 4
CHE	CCL7	360	478	C-C motif chemokine 7
INF	CXCL8	347	34	Interleukin-8 (C-X-C motif chemokine 8)
REC	ALCAM	290	387	CD166 antigen (activated leukocyte cell adhesion molecule)
INF	CSF1	274	114	Macrophage colony-stimulating factor 1
GF	PDGFA	222	243	Platelet-derived growth factor subunit A
REC	TNFRSF10C	205	151	Tumor necrosis factor receptor superfamily member 10C
CHE	CXCL16	195	51	C-X-C motif chemokine 16
REC	FAS	175	51	Tumor necrosis factor receptor superfamily member 6
REC	SCARB2	38	25	Lysosome membrane protein 2 (Scavenger receptor class B member 2)

Abbreviation: hAMSCs, human amniotic membrane-derived mesenchymal stromal cells.

characterized by a high degree of interactions (CCL4/5, CXCL1/5/8/16, and TIMP2), and linked to CCL2/7. The second cluster was defined by less interactor connections (SERPINE1, VEGFA, TGFB1, TIMP1, IL6, CSF1, SPP1, and IGFBP3/4), and linked to IGFBP6, INHBA, and PLAUR (Figure 2).

GO enrichment analysis was performed using the 200 factors as the background data set. When all 37 molecules were sifted, only two GO (biological process [BP]) terms were identified (GO:0043687, post-translational protein modification,  $P$  value  $6.61 \times 10^{-4}$ ; GO:2000501, regulation of natural killer cell chemotaxis,  $9.83 \times 10^{-4}$ ) (Table S2). After having refined the search for the most abundant proteins ( $>10$  ng), we found two BP (GO:0010648, negative regulation of cell communication,  $1.34 \times 10^{-4}$ , GO:0023057, negative regulation of signalling,  $1.34 \times 10^{-4}$ ), defined by the same proteins, and three molecular function (MF) terms (GO:0005520, insulin-like growth factor binding,  $2.74 \times 10^{-4}$ ; GO:0031994, insulin-like growth factor I binding,  $2.74 \times 10^{-4}$ ; GO:0031995, insulin-like growth factor II

binding,  $2.74 \times 10^{-4}$ ), all defined by IGFBP3/4/6 (Table S2). Searching for the less expressed factors ( $<10$  ng), one BP (GO:2000501, regulation of natural killer cell chemotaxis,  $3.33 \times 10^{-4}$ ) and one MF (GO:0042802, identical protein binding,  $8.98 \times 10^{-4}$ ) terms were found to be enriched (Table S2).

Last, GO enrichment was performed on the two clusters identified by functional association analysis. The first cluster allowed for the identification of several BP related to immune cells chemotaxis (GO:0030595, leukocyte chemotaxis,  $2.83 \times 10^{-5}$ ; GO:0030593, neutrophil chemotaxis,  $9.27 \times 10^{-5}$ ; GO:0071621, granulocyte chemotaxis,  $1.14 \times 10^{-4}$ ) and migration (GO:1990266, neutrophil migration,  $1.14 \times 10^{-4}$ ; GO:0097530, granulocyte migration,  $1.68 \times 10^{-4}$ ; GO:0050900, leukocyte migration,  $2.82 \times 10^{-4}$ ), supporting a general influence on cell movement (GO:0060326, cell chemotaxis,  $9.77 \times 10^{-5}$ ) (Table S2). Also, four MF related to receptor binding resulted enriched (Table S2). When the components of the second cluster were analyzed, six BP, mainly related to regulation of cell

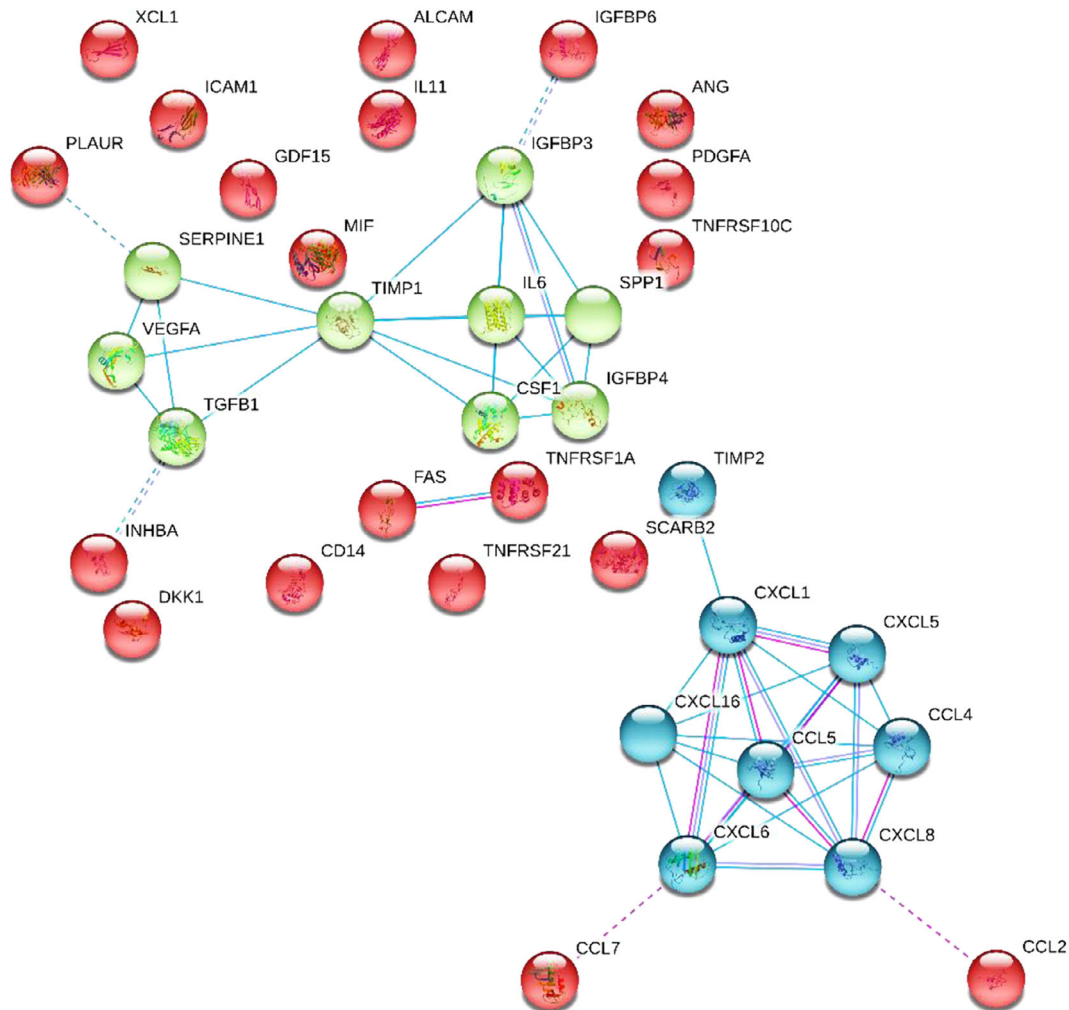


**FIGURE 2** Functional association network for identified secreted factors. Using the online tool STRING, protein-protein interaction levels for 37 proteins of the hAMSCs CM were mined. The blue connections are for proteins with known interactions based on curated databases; red connections for proteins with experimentally determined interactions. Empty nodes, proteins of unknown 3D structure; filled nodes, known or predicted 3D structure. CM, conditioned medium; hAMSCs, human amniotic membrane-derived mesenchymal stromal cells

growth and metabolic processes (GO:0051248, negative regulation of protein metabolic process,  $1.81 \times 10^{-4}$ ; GO:0040008, regulation of growth,  $2.83 \times 10^{-4}$ ) were identified (Table S2). Eventually, one MF was enriched (GO:0001968, fibronectin binding,  $6.87 \times 10^{-4}$ ) (Table S2). As a whole, the combination of functional association and GO enrichment allowed a strong fingerprinting of hAMSCs secreted factors towards immune cell chemotaxis and growth/metabolism.

### 3.3 | hAMSC-EVs miRNAs

Three hundred thirty-six differently expressed miRNAs were detected in EVs. Hierarchical clustering showed a more similar profile for hAMSCs 1 and 3 (Figure 3), albeit correlation analysis again emphasized consistent homogeneity ( $R^2 = 0.94$  for donor 1 vs 2,  $R^2 = 0.95$  for 1 vs 3, and  $R^2 = 0.96$  for 2 vs 3). Thus, an average  $C_{RT}$  value was calculated (Table S3). The most expressed miRNA resulted to be miR-24-3p, followed by miR-146a-5p.

To handle such a large amount of data, consistent with recent reports, even for most abundant MSC EV-miRNAs, there are approximately 1.3 molecules per vesicle,<sup>33</sup> and 100 EVs would be needed to

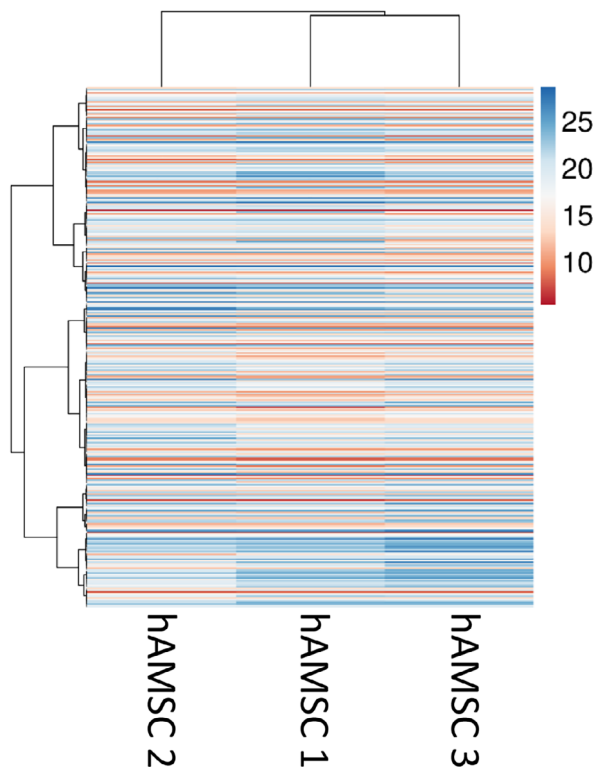


**FIGURE 3** Heat map of hierarchical clustering analysis of the normalized  $C_{RT}$  values of detected miRNAs in the three hAMSC-EVs under study. Rows are centered. The sample clustering tree is shown at the top. The color scale shown in the map illustrates the expression levels of factors, as  $C_{RT}$  values, across all samples: red shades = high expression (low  $C_{RT}$  values) and blue shades = low expression (high  $C_{RT}$  values). EVs, extracellular vesicles; hAMSCs, human amniotic membrane-derived mesenchymal stromal cells

shuttle one copy to a target cell.<sup>34</sup> Since a few thousand MSC-EVs are incorporated per day in several cell types,<sup>35-37</sup> it is presumable that only miRNAs present at least at 1% of most abundant ones might be incorporated with at least one molecule. Therefore, only the first 51 EV-miRNAs, covering 95% of the EVs genetic message, were taken into consideration (Table S3).

Many of the selected miRNAs are predicted to regulate hundreds to thousands of transcripts, with miR-106-5p potentially targeting up to 1433 genes and the two most abundant miRNAs, miR-24-3p and miR-146a-5p, 582 and 413, respectively (Table S4). GO analysis based only on experimentally validated targets identified 144 enriched BP (data not shown), with the vast majority shared by several miRNAs. To obtain a more solid picture, only BP potentially regulated by at least 10 miRNAs were selected. Twenty-three miRNAs were able to define 124 terms, encompassing different BP such as, among others, cell death (GO:0008219, 16 miRNAs), apoptotic process (GO:0006915, 11), cell cycle (GO:0007049, 10), cell differentiation (GO:0030154, 13), cell communication (GO:0007154, 13), developmental process (GO:0032502, 10), immune system development (GO:0002520, 10), gene expression (GO:0010467, 14), and signaling (GO:0023052, 12) (Figure 4). For several of these processes, both positive and negative related terms were found, therefore hindering an unambiguous effect.

Regarding miR-24-3p and miR-146a-5p, accounting for one third of the EV genetic weight, nine enriched BP were shared, including cell death (GO:0008219), apoptotic process (GO:0006915) and five terms related to cell cycle, like regulation of cell cycle (GO:0051726), both positive and negative (GO:0045787/GO:0045786) and cell cycle arrest (GO:0007050) (Figure 5). Experimentally validated transcripts targeted by both miRNAs were analyzed and the following seven emerged: *BRCA1*, *CARD10*, *CCNA2*, *CCND1*, *FAF1*, *NOTCH1*, and *TGFB1*. GO analysis revealed 85 BP (encompassing at least four genes, Table S5), including 20 terms defining metabolic pathways, such as regulation of metabolic process (GO:0019222, 7 genes) of several type of macromolecules such as protein (GO:0051246, 7 genes), nitrogen (GO:0051171, 7 genes), phosphate (GO:0019220, 6 genes), and RNA (GO:0051252, 6 genes). Notably, also regulation of gene expression (GO:0010468, 6 genes), cell cycle (GO:0007049, 5 genes), apoptotic process (GO:0006915, 4 genes), and cell death (GO:0008219, 4 genes) were defined. Nevertheless, in general, unfocused prediction based solely on target genes, without tissue or disease context, led to a heterogeneous picture unable to fully and consistently predict a single miRNA or miRNome effect or therapeutic potency.

### 3.4 | Target and effect prediction of hAMSC-EV miRNAs in the setting of musculoskeletal conditions

Due to the considerations above, we focused our attention on miRNA involved in two widespread musculoskeletal conditions, OA and tendinopathies, both characterized by tissue degeneration and inflammation.





**FIGURE 4** Visualization of the target enriched GO biological processes annotation regulated by EV-miRNAs. Heat map of the target significant and enriched GO BP annotations shared by at least 10 miRNAs among those laying in the 51 most abundant miRNAs. The color scale shown in the map illustrates the significance, as *P* value, for each BP: dark blue = high significance (low *P* value) and light blue = low significance (high *P* value). BP, biological process; EV, extracellular vesicle; GO, gene ontology

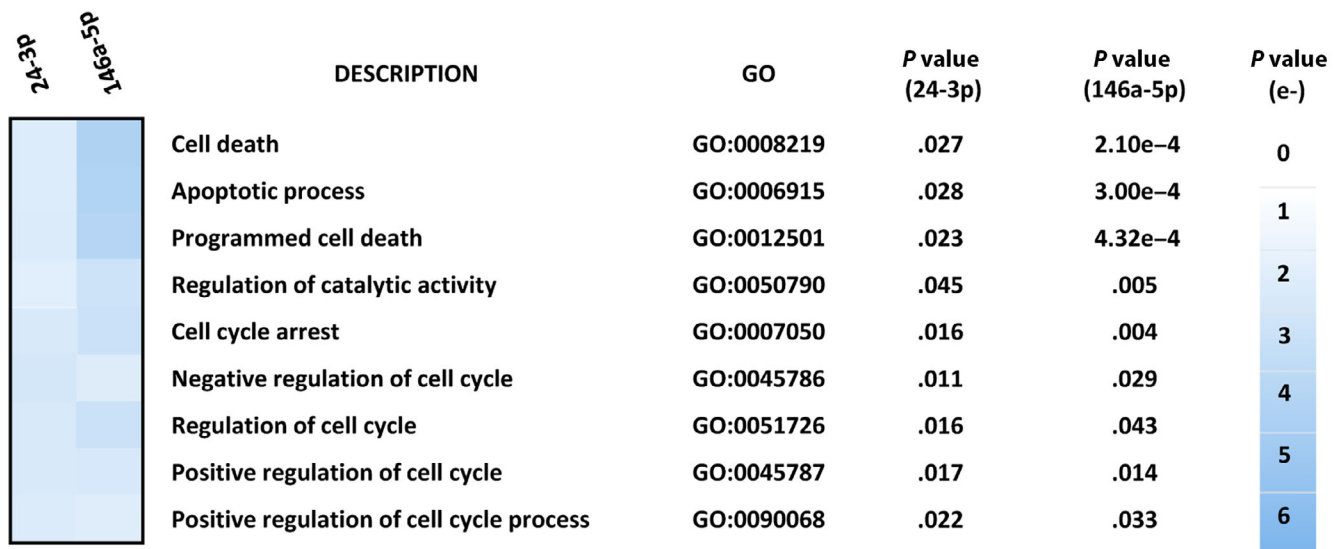


**FIGURE 5** Heat map of the target significant and enriched GO BP annotations shared by the two most abundant hAMSC-EVs miRNAs, miR-24-3p and miR-146a-5p. P values for each GO BP term are shown. The color scale shown in the map illustrates the significance, as P value, for each BP: dark blue = high significance (low P value) and light blue = low significance (high P value). BP, biological process; EV, extracellular vesicle; GO, gene ontology; hAMSCs, human amniotic membrane-derived mesenchymal stromal cells

**TABLE 2** miRNAs involved in cartilage processes

Function	% EV-genetic weight	Target	Role
Protective			
miR-24-3p	17.73	P16INK4A	Senescence
miR-222-3p	4.87	HDAC-4	ECM
miR-125b-5p	2.68	ADAMTS-4	ECM
miR-193b-3p	2.37	TGFB2, TGFB3, MMP-19	Inflammation, ECM
miR-17-5p	1.25	p62/SQSTM1	Autophagy
miR-320-3p	1.09	BMI-1, RUNX2, MMP-13	Viability, ECM
miR-92a-3p	1.04	ADAMTS-4, ADAMTS-5, HDAC2	ECM
miR-210-3p	0.51	DR6, HIF-3 $\alpha$	Apoptosis, ECM
miR-199a-3p	0.39	COX-2	Catabolism
miR-26a-5p	0.30	iNOS, KPNA3	Homeostasis
miR-130a-3p	0.25	TNF $\alpha$	Inflammation
miR-30a-3p	0.23	ADAMTS-5	ECM
miR-149-5p	0.23	TNF $\alpha$	Inflammation
miR-193a-5p	0.19	TGFB2, TGFB3, MMP-19	Inflammation, ECM
Total	33.12		
Destructive			
miR-21-5p	3.81	GDF-5	Chondrogenesis
miR-30b-5p	1.96	BECN1, ATG5	Apoptosis, ECM
miR-34a-5p	0.55	SIRT1	Apoptosis
miR-16-5p	0.30	SMAD3	ECM
miR-181a-5p	0.21	ZNF440	Inflammation
Total	6.85		
Pro/Des			
miR-146a-5p	16.41	TRAF6/SMAD4	Proliferation/Early OA
miR-145-5p	1.02	TNFRSF11B/SOX9, SMAD3	Proliferation/ECM
Total	17.43		

Abbreviations: ECM, extracellular matrix; EVs, extracellular vesicles.

**TABLE 3** miRNAs involved in tendon processes

Function	% EV-genetic weight	Target	Role
Protective			
miR-146a-5p	16.41	IRAK1, TRAF6	Inflammation
miR-193b-3p	2.37	COL2, ACAN, SOX5, MAPK, IRF1, IRAK1, NF- $\kappa$ B	Inflammation, ECM
miR-100-5p	2.32	NF- $\kappa$ B, MAPK, IL-6R, PTK2	Inflammation, proliferation
miR-145-5p	1.02	JAK/STAT pathway	Inflammation
miR-29a-3p	0.82	IL-33	Inflammation, ECM
miR-181a-5p	0.21	IFN- $\gamma$ , MAPK1, IL-5, IRAK1	Inflammation, oxidative stress
Total	23.15		

Abbreviations: ECM, extracellular matrix; EVs, extracellular vesicles.

**TABLE 4** miRNAs involved in T lymphocyte activation and polarization

Function	% EV-genetic weight	Role
T cell related		
miR-146a-5p	16.41	Inhibition
miR-125b-5p	2.68	Inhibition
Total	19.09	
IFN- $\gamma$ related		
miR-24-3p	17.73	Downregulation
miR-29a-3p	0.82	Downregulation
miR-181a-5p	0.21	Downregulation
Total	18.76	
Treg favoring		
miR-146a-5p	16.41	Inhibit STAT1 stabilization/ downregulates IFN $\gamma$ transcription
miR-99a-5p	2.39	Reduce mTOR expression
miR-10a-5p	0.21	Repression of Bcl-6 expression
Total	19.00	
Treg inhibiting		
miR-31-3p	0.18	Inhibit iTreg polarization
miR-92a-3p	1.04	Inhibit iTreg polarization
miR-17-5p	1.25	Inhibit iTreg polarization
Total	2.47	

Abbreviation: EV, extracellular vesicle; mTOR, mammalian target of rapamycin.

By comparing the top 51 EV-miRNAs with miRNAs reported to be involved in OA pathogenesis,<sup>38</sup> 14 protective and 5 destructive miRNAs were identified (Table 2). As a whole, protective miRNAs, including miR-24-3p, represented 33.12% of EVs genetic weight vs the 6.85% represented by the destructive ones. Notably, two miRNAs associated with a dual role in OA cartilage were present (17.43%), with miR-146a-5p (16.41%) being the most abundant.

Performing the same comparison with miRNAs recently discovered to be involved in tendon homeostasis and tendinopathies,<sup>39,40</sup>

**TABLE 5** miRNAs involved in macrophage polarization

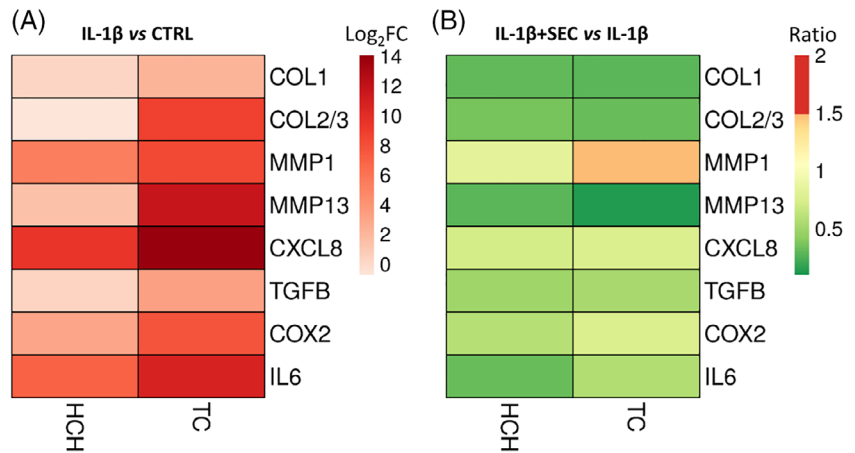
Function	% EV-genetic weight	Role
M1 related		
miR-125b-5p	2.67	Pro M1
miR-145-5p	1.02	Pro M1
miR-130a-3p	0.25	Pro M1, anti M2
Total	3.94	
M2 related		
miR-24-3p	17.73	Pro M2, anti M1
miR-146a-5p	16.41	Pro M2, anti M1
miR-222-3p	4.87	Pro M2
miR-34a-5p	0.55	Pro M2
miR-181a-5p	0.21	Pro M2, anti M1
Total	39.78	

Abbreviation: EV, extracellular vesicle.

six were found involved in homeostasis and healing (Table 3), including miR-146a-5p, and as a whole they represented 23% of the EV genetic weight. Intriguingly, in a fragmented patchwork of MFs, all six miRNAs were outlined to be involved in inflammatory processes, and their downregulation during tendon injuries linked with an increase of inflammatory signaling.

A closer look at T lymphocytes and macrophages, both active players in OA and tendinopathy,<sup>41,42</sup> revealed 10 miRNAs that play a relevant role in modulating proliferation, activation, and differentiation towards the inflammatory T helper-1 (Th1) subset, or directly involved in modulating the polarization of CD4<sup>+</sup> T lymphocytes towards the regulatory T-cell subset (Table 4). In particular, miR-146a-5p and miR-125b-5p, that encompassed 19% of the EV weight, were shown to be involved in the negative regulation of T lymphocyte proliferation and activation. Three (18.76%) were shown to be directly involved in the downregulation of IFN $\gamma$  expression, where miR-24-3p (17.73%) represented the main contributor. Furthermore, six miRNAs were reported to modulate Treg homeostasis, three of which (19%; predominantly miR-146a-5p with 16.41%) favor Treg while the other three (2.47%) inhibit Treg.

**FIGURE 6** hAMSC secretome effect on inflamed chondrocytes and tenocytes. A, Chondrocytes (HCH) and tenocytes (TC) were treated with 1 ng/mL IL-1 $\beta$  for 48 hours, and for the indicated transcripts the Log<sub>2</sub> Fold Change (FC) vs CTRL is shown. B, hAMSC secretome (SEC) was administered together with 1 ng/mL IL-1 $\beta$ , and the IL-1 $\beta$  + SEC vs IL-1 $\beta$  Ratio is shown. For both panels, averaged values from three independent donors, each assayed in technical duplicate, are presented. The color scale shown in the heat maps illustrates the expression levels as Log<sub>2</sub>FC for panel (A) and ratio for panel (B). hAMSCs, human amniotic membrane-derived mesenchymal stromal cells



Five miRNAs involved in M2 and three involved in M1 phenotype regulation were identified (Table 5).<sup>43</sup> The presence of miR-24-3p and miR-146a-5p, responsible for the M1 to M2 switch, and miR-222-3p, involved in the control of M2 polarization, tips the balance toward a more pronounced influence on M2 phenotype. As a whole, the weight of M2-related miRNAs was 40% vs 4% for M1-related miRNAs.

### 3.5 | Functional analysis of the effect of the hAMSC secretome on inflamed chondrocytes and tenocytes

Several of the secreted factors and EV-embedded miRNAs suggest anti-inflammatory and regenerative features of the hAMSC secretome on immune cells, chondrocytes or tenocytes. A well-consolidated amount of data has already demonstrated the net anti-inflammatory and phenotype-switch outcomes on immune cells (see Section 4). For this reason, to validate bioinformatics, we focused our attention on chondrocytes and tenocytes that were treated for 48 hours with 1 ng/mL IL-1 $\beta$ , and markers reported to be involved in matrix remodeling (COL1, COL2 for chondrocytes and COL3 for tenocytes, MMP1 and MMP13) and inflammation (CXCL8, TGFB, COX2, and IL-6) were tested by qRT-PCR (Figure 6A). As expected, IL-1 $\beta$  treatment resulted in a consistent modulation of the analyzed genes, and tenocytes had a stronger response for both inflammatory and matrix markers when compared to chondrocytes. When the hAMSC secretome was administered together with the inflammatory stimulus, a trend toward inflammation reduction emerged (Figure 6B), with both cell types behaving similarly, and confirming our bioinformatics prediction.

## 4 | DISCUSSION

Herein we characterized an array of 200 soluble factors and a panel of 754 miRNAs in the hAMSC secretome and EVs, respectively. Several of these molecules are involved in immune-related and tissue restoration processes, therefore in accordance with in vitro and preclinical results observed with hAMSCs and their secretome. As per

our scientific interest, data were analyzed in view of the possibility to treat musculoskeletal conditions such as OA and tendinopathy, paving the way for a broader use of hAMSCs or their secretome in similar clinical applications.

Many of the most abundant secreted factors are involved in the remodeling and homeostasis of the extracellular matrix (ECM) that is heavily altered in both OA and tendinopathies.<sup>44,45</sup> We found high levels of tissue inhibitor of metalloproteinases 1 and 2 (TIMP1 and TIMP2) in the hAMSC secretome. TIMP levels were reported by others to decrease in diseased tendons of rabbits,<sup>46</sup> and the expression of TIMP1 was shown to inhibit ECM degradation by metalloproteinase 2 (matrix metallo proteinase 2, MMP2).<sup>47</sup> Moreover, administration of MMP inhibitors was shown to reduce collagen degradation after rotator cuff damage in rats,<sup>48</sup> and to favor tendon-bone healing in chronic tendinosis in humans.<sup>49</sup> Similarly, in damaged cartilage, TIMPs regulate ECM remodeling by directly inhibiting MMPs.<sup>44</sup> Also, in a canine model, TIMP2 was described to be poorly expressed in both OA cartilage<sup>50</sup> and synovial fluids.<sup>51</sup> Other abundant secretome factors involved in ECM remodeling are SERPINE1 and PLAUR. SERPINE1 is a master suppressor of proteases and is transiently upregulated after tendon injury<sup>52</sup> to balance matrix remodeling and to mediate fibrotic adhesions by suppressing MMP activity.<sup>53</sup> SERPINE1 was reported to have a similar role in ECM homeostasis in OA, where SERPINE1 levels positively correlated with cartilage synthesis<sup>54</sup> and counteracted urokinase/tissue-type plasminogen activators (uPA/tPA), found to be elevated in OA cartilage.<sup>55</sup> PLAUR also controls uPA activity and, consistent with a role in ECM remodeling, is transiently upregulated during Achilles tendon healing in rats.<sup>56</sup> PLAUR was described to reduce plasminogen activation in plasmin, which in turns activates MMPs degrading cartilage structure.<sup>57</sup> Altogether, ECM-related factors in the hAMSC secretome have a protective and healing role in both cartilage and tendons.

Notably, the three most abundant factors, insulin-like growth factor-binding proteins (IGFBPs) 4/6/3, whose role is mainly due to the ability to bind IGF1, are also linked with ECM. In fact, in both tendons<sup>58</sup> and cartilage,<sup>59</sup> IGF1 stimulates ECM synthesis and cell proliferation, and IGFBPs regulate IGF1 bioavailability and activity by reducing IGF1R-dependent sequestration and also protecting IGF1

from pericellular proteases.<sup>60</sup> Therefore, increased IGFBP levels may prolong its positive effect. In this frame, in a collagenase tendinopathy model in horses, local IGFbps,<sup>61</sup> as well as IGF1,<sup>62</sup> increased during repair. This paradigm may be of particular importance since increased levels of circulating IGF1 do not entail their biological action locally at the tendon, but rather only local IGF1 can stimulate and regulate collagen synthesis in tendon tissue.<sup>63</sup> Similarly, IGFbps bind chondrocyte-secreted IGF1 and induce the production of cartilage ECM ultimately exerting a protective role in OA.<sup>64</sup> Moreover, IGFbps are normally localized within the fibronectin network in cartilage ECM thus creating reservoirs of IGF1 with important roles in cartilage homeostasis and repair.<sup>65</sup> Therefore, local administration of the hAMSC secretome may provide exogenous IGFbps to create ECM complexes containing fibronectin and IGF1 in both cartilage and tendons.

Nevertheless, few molecules potentially harmful for both cartilage and tendons, such as IL6 and TGF $\beta$ , were detected. IL6 is a pleiotropic pro-inflammatory cytokine able to increase MMPs levels and is found in OA synovial fluid and surrounding tissues.<sup>66</sup> Accordingly, IL6 intra-articular injections was described to reproduce OA-like cartilage lesions in mice.<sup>67</sup> Similarly, TGF $\beta$  is a key fibrotic mediator,<sup>68</sup> whose administration may lead to an increased fibrotic phenotype with reduced mechanical strength. Also, TGF $\beta$  supplementation as OA therapeutic induced inflammation, synovial hyperplasia, and osteophyte formation.<sup>69</sup> Therefore, a careful balance of protective and damaging factors for tendons and cartilage must be considered, although protective molecules are preponderant.

As a whole, hAMSCs secreted factors defined several GO annotations connected with immune cell motility and chemotaxis, shaped by CXCL1/5/8/16 and CCL2/4/5/7. This is in agreement with proteomic analysis reports on adipose-derived mesenchymal stem/stromal cells (ASCs), bone marrow-derived mesenchymal stem/stromal cells (BMSCs), and Wharton's Jelly-derived mesenchymal stem/stromal cells (WJMSCs) secretomes,<sup>29,70,71</sup> suggesting a conserved capacity for MSCs of different origin. Regarding CXC-chemokines members, CXCL1/5/8 are classified as inflammatory, and CXCL16 as both inflammatory and homeostatic.<sup>72</sup> Neutrophils are the main responsive cell type since they express CXCR1/CXCR2 receptors.<sup>73</sup> Interestingly, neutrophils are hardly found in chronic synovitis,<sup>74</sup> whereas, in the early inflammatory phase of tendinopathies they transiently accumulate to remove debris and release a second wave of cytokines that transition the healing process into proliferation and remodeling.<sup>75</sup> The major target cells of CC-chemokine members such as CCL2/4/5/7 are monocytes/macrophages and T cells,<sup>72</sup> supporting the general monocyte/macrophage chemo-attractive capacity of MSC-secretome.<sup>70</sup> Eventually, the presence of CSF1, by reinforcing differentiation and survival of monocytes/macrophages and anti-inflammatory M2 polarization,<sup>76</sup> corroborates the hAMSC secretome-dependent decrease of M1 and increase of M2 polarization.<sup>78</sup> These results confirm the actions of the hAMSC secretome on several immune cell populations.<sup>4</sup>

The profound influence on the immune system emerged also for EV-miRNAs. Among the most abundant hAMSCs-EVs miRNAs, many are closely related with T cells and macrophage function/polarization. Both CD4/CD8<sup>77</sup> and inflammatory Th1 lymphocytes<sup>78</sup> have been

isolated from synovial biopsies of OA patients. Similar results were reported in almost all stages of tendinopathy.<sup>79</sup> miR146a-5p regulates CD4 and CD8 survival and inhibits activation,<sup>80</sup> and similarly miR-125b is a negative regulator of T-cell function and maintains CD4 T lymphocytes in a naïve state.<sup>81</sup> Other relevant highly represented EV-miRNAs, such as miR-24-3p and miR-181a-5p, target IFN $\gamma$  expression in CD4 lymphocytes,<sup>82,83</sup> while miR-29a-3p also affects differentiation toward inflammatory Th1.<sup>84</sup> Furthermore, Treg are also involved in the inflammatory status in both OA and tendinopathy.<sup>85,86</sup> Herein, six of the identified miRNAs were found to be able to modulate Treg polarization and stabilization. miR-146a-5p contrasts the polarization toward inflammatory Th1,<sup>87</sup> miR-99a-5p affects inducible Treg polarization by targeting mammalian target of rapamycin (mTOR),<sup>88</sup> and miR-10a-5p also targets Treg by stabilizing the expression of FoxP3.<sup>89</sup> Overall, the genetic weight of miRNAs favoring Treg polarization far exceeded that of contrasting miRNAs, supporting what previously observed using hAMSCs and their secretome in toto.<sup>7,16</sup> Similarly, the genetic weight of M2-polarizing EV-miRNAs, such as miR-24-3p, miR-146a-5p, and miR-222-3p, resulted much larger than M1-inducing miRNAs. In particular, miR-24-3p mediates the M1 to M2 transition, and enhances the ability of IL-4 and IL-13 to generate a M2 phenotype.<sup>90</sup> miR-24-3p is also a negative regulator of toll-like receptor (TLR)-mediated pro-inflammatory cytokine production in M1 macrophages.<sup>91</sup> miR-146a-5p has been reported to be higher in M2 polarized macrophages and able to promote M2 polarization.<sup>92</sup> Furthermore, miR-222-3p has been shown to reduce the amount of SOCS3, a negative regulator of M2 promoter STAT3.<sup>93</sup> This is in line with the previously reported ability of hAMSC-EVs to favor M2 macrophage polarization in an induced OA model, ultimately enhancing pain tolerance with an almost complete restoration of cartilage.<sup>94</sup>

Therefore, EV-miRNAs are involved in a specific regulation of tissue regeneration that goes beyond inflammation control. The two most abundant miRNAs, miR-146a-5p and miR-24-3p, are involved in regulating OA matrix remodeling. Mir-146a-5p is a crucial determinant in OA associated knee joint homeostasis and pain symptoms, maintaining the balance between inflammatory response and expression of pain factors in cartilage and synovium.<sup>95</sup> Early on in OA, cartilage miR-146a-5p expression is increased by IL-1 $\beta$  and plays a key role in catabolic factor inhibition. Conversely, in severe OA its expression is reduced, leading to progressive degradation of the cartilage due to decreased suppression of catabolic signals.<sup>96</sup> In fact, MMP3 levels have been reported to be negatively associated with miR-146a-5p expression, while type II collagen and aggrecan were positively associated, pinpointing a novel role of miR-146a-5p in driving cartilage degeneration.<sup>97</sup> miR-24-3p, that is downregulated in OA tissues, targets p16INK4a which accumulates and enhances senescence and cartilage catabolism.<sup>98</sup> Consistently, miR-24-3p promotes the proliferation and inhibits the apoptosis of rat chondrocytes.<sup>99</sup> We also found miRNAs involved in ECM protection, namely miR-222-3p, miR-125b-5p, and miR-193b-3p.<sup>38</sup> Together with miR-146a-5p and miR-24-3p and other less-expressed miRNAs, they could confer hAMSCs EV-miRNAs a cartilage protection role. Similarly, several miRNAs are involved in protective mechanisms counteracting inflammation and ECM degeneration

after tendon injury, where the role of miRNA is, at present, less deciphered. Again, miR-146a-5p results a crucial player due to its anti-inflammatory activity. In patients with shoulder tendinopathy and glenohumeral arthritis, the downregulation of miR-146a-5p has been shown to be associated with the severity of inflammation.<sup>40</sup> Similar downregulation during tendinopathy was also observed for miR-193b-3p and miR-100-5p, the former of which is associated with both inflammatory signaling and ECM,<sup>40,100</sup> whereas downregulation of the latter, considering its role in the regulation of cell growth and proliferation,<sup>40</sup> might delay repair and favor the persistence of tissue damage.

In previous work, we have shown that factors secreted by hAMSCs are able to suppress the proliferation, inflammatory cytokine production, and functions of T lymphocytes,<sup>7,16,17</sup> monocytes,<sup>8</sup> dendritic cells,<sup>5</sup> macrophages,<sup>8</sup> and are able to induce a phenotype and functional switch of monocytes toward macrophages with anti-inflammatory pro-regenerative M2-like features,<sup>7,8</sup> and also support the expansion of regulatory T cells.<sup>7,16</sup> More recently, we demonstrated that hAMSC-secreted factors suppress B-cell proliferation and differentiation, with an increase of mature B cells and a reduction of antibody-secreting cells.<sup>101</sup> Similar findings were obtained also by Li et al on natural killer cells.<sup>6</sup> The efficacy of hAMSC and their secreted factors was also confirmed in vivo in several animal models of diseases where the inflammatory component plays a prevalent role such as lung<sup>102-106</sup> and liver<sup>107</sup> fibrosis, wound healing,<sup>8,108,109</sup> multiple sclerosis,<sup>110</sup> inflammatory bowel disease,<sup>110</sup> colitis,<sup>110,111</sup> sepsis,<sup>110</sup> traumatic brain injury,<sup>112</sup> Huntington's disease,<sup>18</sup> arthritis,<sup>11,110,113</sup> and tendinopathy.<sup>12,13</sup> Herein, the bioinformatics analysis performed in our study support the largely experimentally validated results obtained both in vitro and in vivo for the immune regulation.

Regarding cartilage and tendon cells which are of particular interest in this study, the literature currently lacks functional in vitro tests directly assessing the ability of hAMSCs or their secretome to suppress inflammation and promote regenerative features such as restoring the baseline levels of altered matrix components (eg, collagen) or matrix modifying enzymes (eg, MMPs). Herein, in a model of inflammation relying on IL-1 $\beta$  and largely used to treat chondrocytes<sup>114</sup> and tenocytes,<sup>115</sup> we observed that hAMSC secretome was able to promote a trend toward restoration of homeostatic levels for both inflammation and ECM remodeling markers altered by the inflammatory stimulus. This is of crucial relevance since ECM alteration is orchestrated by both dysregulation of collagen deposition and structure and increase of MMPs which degrade major ECM structural components, such as aggrecan and collagen.<sup>116</sup> Thus, gene expression results obtained from the in vitro model of inflamed chondrocytes and tenocytes support the bioinformatics prediction for the targeting of inflammation and ECM degeneration related players.

Eventually, beyond the molecular explanation of hAMSCs secretome anti-inflammatory and regenerative properties, the identified molecules might also be a milestone for the future development of potency and release assays to fingerprint clinical-grade batches of whole secretome or purified components. In fact, due to the diversity of MSC-based medicinal products at the level of cell source, manufacturing process and indication, specific fingerprint signatures

are needed to ensure their quality and guide their use. To date, few minimal criteria for defining MSCs and good manufacturing practice (GMP)-MSCs have been proposed.<sup>25,117</sup> However, no concluding recommendations regarding potency assays are provided, since every MSC product, both cell-based or cell-free, is unique and quality control assays should be developed on a case-by-case and therapeutic application basis. In this frame, future experiments that associate the presence/abundance of herein identified molecules, both as single players or as a disease-driven multifactorial panel, with the modulation of related gene/pathway targets, will pave the way for the development of initial and quick screening to either integrate or guide decision-making on the implementation of more demanding potency assays, such as immune cell inhibition or suppressor cell activation.<sup>118</sup> Furthermore, for pathologies such as OA or tendinopathy where potency assays are missing, immunoregulatory or tissue-protective cytokines or miRNAs presented in this study might be a milestone for the future development of disease-targeted potency assays since the relevance and acceptability of the chosen potency readout largely depends on the clinical indication. As an example, EV-enriched miR-320-3p and miR-199a-3p are direct regulators of *MMP13* and *COX2* mRNAs, respectively, and both were downregulated after treatment with the hAMSC secretome, although to rule out a direct relationship between the two, further experiments will be necessary. Therefore, after a rigorous validation of a direct miRNA/mRNA or cytokine/pathway interaction for a few and selected players through functional tests, as the one herein proposed or those previously published for immune cells, disease-related ELISA and qRT-PCR assays performed on the secretome or EVs might define a new time/cost-effective front line of future standard set of assays that could be used as "release criteria" per se or as first line of screening to proceed or not with more sophisticated and time-consuming/costly techniques for hAMSCs and/or their cell-free products for clinical use.

The presented study has some limitations. The number of assayed secreted factors was limited as well as the number of miRNAs, with several others potentially involved in inflammation, tendinopathy, or OA. Especially for tendon diseases, to date, only a few factors or miRNAs have been associated with the pathology or healing, and mainly sifted for protective roles leaving degenerative players underestimated. Also, the functional test used herein relied on an in vitro model with an IL-1 $\beta$  concentration quite far from in vivo conditions in terms of load of insult, thus possibly altering/hindering a finely tuned response of cells. Furthermore, we focused on a limited panel of targets that should be increased in number and further validated by specific miRNA-mRNA interaction and augmentation/depletion-vs-effect assays and eventually on the protein level. However, this work reports consistent insights to explain and interpret the therapeutic effects of hAMSCs and their secretome observed in both in vitro and preclinical studies.

## 5 | CONCLUSIONS

In this report, we shed light on hAMSCs secreted factors and EV-embedded miRNAs to heal inflamed and diseased joints and tendons,

supporting in vitro and preclinical results. Further studies will be necessary to describe in more detail the secretome at proteomic, lipidomic, or nucleic acid levels in order to better predict and translate the overall potency of this cell-free clinical product in joint diseases at first, and in the wide array of pathologies that could potentially benefit from the off-the-shelf hAMSCs cell-free products.

## ACKNOWLEDGMENTS

This work was supported by the Italian Ministry of Health, “Ricerca Corrente”; Fondazione Poliambulanza of Brescia; the Italian Ministry of Health, MIUR (5x1000 year 2017); intramural funds from the Università Cattolica del Sacro Cuore (“Linea D1-2018” and “Linea D1-2019”); and PRIN 2017 program of Italian Ministry of Research and University (MIUR) Grant 2017RSAFK7 to O.P. The authors thank physicians and midwives of Department of Obstetrics and Gynecology of Fondazione Poliambulanza-Istituto Ospedaliero, Brescia, Italy, and all of mothers who donated placenta. The authors acknowledge Regenerative Medicine Research Center (CROME) of Università Cattolica del Sacro Cuore. This work contributes to COST Action CA17116 International Network for Translating Research on Perinatal Derivatives into Therapeutic Approaches (SPRINT), supported by COST (European Cooperation in Science and Technology).

## CONFLICT OF INTEREST

The authors declared no potential conflicts of interest.

## AUTHOR CONTRIBUTIONS

E.R., A.P.: conception and design, collection and assembly of data, data analysis and interpretation, manuscript writing; C.P.O., A.R.S.: collection and assembly of data, data analysis and interpretation; A.C.: provision of study material; M.V.: statistical analysis; F.L.: collection and assembly of data; O.P., L.d.G.: financial support, final approval of manuscript.

## DATA AVAILABILITY STATEMENT


All data are available in the main text or Supporting Information and tables.

## ETHICS STATEMENT

The study was conducted in accordance with Helsinki Declaration. Informed written consent was obtained from specimen donors, according to Comitato Etico Provinciale of Brescia, Italy (NP2243, January 19, 2016).

## ORCID

Enrico Ragni  <https://orcid.org/0000-0003-0272-7417>

Carlotta Perucca Orfei  <https://orcid.org/0000-0001-6162-8668>

Antonietta Rosa Silini  <https://orcid.org/0000-0001-6208-3583>

Marco Viganò  <https://orcid.org/0000-0002-6463-6564>

## REFERENCES

- Saeedi P, Halabian R, Imani Fooladi AA. A revealing review of mesenchymal stem cells therapy, clinical perspectives and modification strategies. *Stem Cell Investig.* 2019;6:34. <https://doi.org/10.21037/sci.2019.08.11>.
- Wang M, Yuan Q, Xie L. Mesenchymal stem cell-based immunomodulation: properties and clinical application. *Stem Cells Int.* 2018;2018:3057624. <https://doi.org/10.1155/2018/3057624>.
- Kabat M, Bobkov I, Kumar S, Grumet M. Trends in mesenchymal stem cell clinical trials 2004-2018: is efficacy optimal in a narrow dose range? *STEM CELLS TRANSLATIONAL MEDICINE.* 2020;9:17-27. <https://doi.org/10.1002/sctm.19-0202>.
- Silini AR, Magatti M, Cargnoni A, Parolini O. Is immune modulation the mechanism underlying the beneficial effects of amniotic cells and their derivatives in regenerative medicine? *Cell Transplant.* 2017;26:531-539. <https://doi.org/10.3727/096368916X693699>.
- Magatti M, Caruso M, De Munari S, et al. Human amniotic membrane-derived mesenchymal and epithelial cells exert different effects on monocyte-derived dendritic cell differentiation and function. *Cell Transplant.* 2015;24:1733-1752. <https://doi.org/10.3727/096368914X684033>.
- Li J, Koike-Soko C, Sugimoto J, Yoshida T, Okabe M, Nikaido T. Human amnion-derived stem cells have immunosuppressive properties on NK cells and monocytes. *Cell Transplant.* 2015;24:2065-2076. <https://doi.org/10.3727/096368914X685230>.
- Pianta S, Magatti M, Vertua E, et al. Amniotic mesenchymal cells from pre-eclamptic placentae maintain immunomodulatory features as healthy controls. *J Cell Mol Med.* 2016;20:157-169. <https://doi.org/10.1111/jcmm.12715>.
- Magatti M, Vertua E, De Munari S, et al. Human amnion favours tissue repair by inducing the M1-to-M2 switch and enhancing M2 macrophage features. *J Tissue Eng Regen Med.* 2017;11:2895-2911. <https://doi.org/10.1002/term.2193>.
- Topoluk N, Steckbeck K, Siatkowski S, Burnikel B, Tokish J, Mercuri J. Amniotic mesenchymal stem cells mitigate osteoarthritis progression in a synovial macrophage-mediated in vitro explant coculture model. *J Tissue Eng Regen Med.* 2018;12:1097-1110. <https://doi.org/10.1002/term.2610>.
- Li F, Chen YZ, Miao ZN, Zheng SY, Jin J. Human placenta-derived mesenchymal stem cells with silk fibroin biomaterial in the repair of articular cartilage defects. *Cell Reprogram.* 2012;14:334-341. <https://doi.org/10.1089/cell.2012.0002>.
- Vines JB, Aliprantis AO, Gomoll AH, Farr J. Cryopreserved amniotic suspension for the treatment of knee osteoarthritis. *J Knee Surg.* 2016;29:443-450. <https://doi.org/10.1055/s-0035-1569481>.
- de Girolamo L, Morlin Ambra LF, Perucca Orfei C, et al. Treatment with human amniotic suspension allograft improves tendon healing in a rat model of collagenase-induced tendinopathy. *Cell.* 2019;8:1411. <https://doi.org/10.3390/cells8111411>.
- Nicodemo MC, Neves LR, Aguiar JC, et al. Amniotic membrane as an option for treatment of acute achilles tendon injury in rats. *Acta Cir Bras.* 2017;32:125-139. <https://doi.org/10.1590/s0102-865020170205>.
- Eleuteri S, Fierabracci A. Insights into the secretome of mesenchymal stem cells and its potential applications. *Int J Mol Sci.* 2019;20:4597. <https://doi.org/10.3390/ijms20184597>.
- Witwer KW, Van Balkom BWM, Bruno S, et al. Defining mesenchymal stromal cell (MSC)-derived small extracellular vesicles for therapeutic applications. *J Extracell Vesicles.* 2019;8:1609206. <https://doi.org/10.1080/20013078.2019.1609206>.
- Pianta S, Bonassi Signoroni P, Muradore I, et al. Amniotic membrane mesenchymal cells-derived factors skew T cell polarization toward Treg and downregulate Th1 and Th17 cells subsets. *Stem Cell Rev.* 2015;11:394-407. <https://doi.org/10.1007/s12015-014-9558-4>.
- Rossi D, Pianta S, Magatti M, Sedlmayr P, Parolini O. Characterization of the conditioned medium from amniotic membrane cells: prostaglandins as key effectors of its immunomodulatory activity. *PLoS One.* 2012;7:e46956. <https://doi.org/10.1371/journal.pone.0046956>.

18. Giampà C, Alvino A, Magatti M, et al. Conditioned medium from amniotic cells protects striatal degeneration and ameliorates motor deficits in the R6/2 mouse model of Huntington's disease. *J Cell Mol Med.* 2019;23:1581-1592. <https://doi.org/10.1111/jcmm.14113>.
19. Philip J, Hackl F, Canseco JA, et al. Amnion-derived multipotent progenitor cells improve achilles tendon repair in rats. *Eplasty.* 2013;13:e31.
20. Gellhorn AC, Han A. The use of dehydrated human amnion/chorion membrane allograft injection for the treatment of tendinopathy or arthritis: a case series involving 40 patients. *PM R.* 2017;9:1236-1243. <https://doi.org/10.1016/j.pmrj.2017.04.011>.
21. Zhang Z, Zeng L, Yang J, Guo L, Hou Q, Zhu F. Amniotic membrane-derived stem cells help repair osteochondral defect in a weight-bearing area in rabbits. *Exp Ther Med.* 2017;14:187-192. <https://doi.org/10.3892/etm.2017.4497>.
22. Lange-Consiglio A, Perrini C, Tasquier R, et al. Equine amniotic microvesicles and their anti-inflammatory potential in a tenocyte model in vitro. *Stem Cells Dev.* 2016;25:610-621. <https://doi.org/10.1089/scd.2015.0348>.
23. Lange-Consiglio A, Lazzari B, Perrini C, et al. MicroRNAs of equine amniotic mesenchymal cell-derived microvesicles and their involvement in anti-inflammatory processes. *Cell Transplant.* 2018;27:45-54. <https://doi.org/10.1177/0963689717724796>.
24. Ragni E, Perucca Orfei C, Silini AR, et al. miRNA reference genes in extracellular vesicles released from amniotic membrane-derived mesenchymal stromal cells. *Pharmaceutics.* 2020;12:347. <https://doi.org/10.3390/pharmaceutics12040347>.
25. Dominici M, Le Blanc K, Mueller I, et al. Minimal criteria for defining multipotent mesenchymal stromal cells. The International Society for Cellular Therapy position statement. *Cytotherapy.* 2006;8:315-317. <https://doi.org/10.1080/14653240600855905>.
26. Eden E, Navon R, Steinfeld I, Lipson D, Yakhini Z. GOrilla: a tool for discovery and visualization of enriched GO terms in ranked gene lists. *BMC Bioinformatics.* 2009;10:48. <https://doi.org/10.1186/1471-2105-10-48>.
27. Théry C, Witwer KW, Aikawa E, et al. Minimal information for studies of extracellular vesicles 2018 (MISEV2018): a position statement of the International Society for Extracellular Vesicles and update of the MISEV2014 guidelines. *J Extracell Vesicles.* 2018;7:1535750. <https://doi.org/10.1080/20013078.2018.1535750>.
28. Ramos TL, Sánchez-Abarca LI, Muntión S, et al. MSC surface markers (CD44, CD73, and CD90) can identify human MSC-derived extracellular vesicles by conventional flow cytometry. *Cell Commun Signal.* 2016;14:2. <https://doi.org/10.1186/s12964-015-0124-8>.
29. Ragni E, Perucca Orfei C, De Luca P, et al. Secreted factors and EV-miRNAs orchestrate the healing capacity of adipose mesenchymal stem cells for the treatment of knee osteoarthritis. *Int J Mol Sci.* 2020;21:1582. <https://doi.org/10.3390/ijms21051582>.
30. D'Haene B, Mestdagh P, Hellemans J, et al. miRNA expression profiling: from reference genes to global mean normalization. *Methods Mol Biol.* 2012;822:261-272. [https://doi.org/10.1007/978-1-61779-427-8\\_18](https://doi.org/10.1007/978-1-61779-427-8_18).
31. Webber J, Clayton A. How pure are your vesicles? *J Extracell Vesicles.* 2013;2:19861-19866. <https://doi.org/10.3402/jev.v2i0.19861>.
32. Barilani M, Peli V, Cherubini A, Dossena M, Dolo V, Lazzari L. NG2 as an identity and quality marker of mesenchymal stem cell extracellular vesicles. *Cell.* 2019;8:1524. <https://doi.org/10.3390/cells8121524>.
33. Toh WS, Lai RC, Hui JHP, Lim SK. MSC exosome as a cell-free MSC therapy for cartilage regeneration: implications for osteoarthritis treatment. *Semin Cell Dev Biol.* 2017;67:56-64. <https://doi.org/10.1016/j.semcdb.2016.11.008>.
34. Chevillet JR, Kang Q, Ruf IK, et al. Quantitative and stoichiometric analysis of the microRNA content of exosomes. *Proc Natl Acad Sci USA.* 2014;111:14888-14893. <https://doi.org/10.1073/pnas.1408301111>.
35. Ragni E, Banfi F, Barilani M, et al. Extracellular vesicle-shuttled mRNA in mesenchymal stem cell communication. *STEM CELLS.* 2017; 35:1093-1105. <https://doi.org/10.1002/stem.2557>.
36. Ragni E, Perucca Orfei C, De Luca P, et al. Interaction with hyaluronan matrix and miRNA cargo as contributors for in vitro potential of mesenchymal stem cell-derived extracellular vesicles in a model of human osteoarthritic synoviocytes. *Stem Cell Res Ther.* 2019;10:109. <https://doi.org/10.1186/s13287-019-1215-z>.
37. Ragni E, Palombella S, Lopa S, et al. Innovative visualization and quantification of extracellular vesicles interaction with and incorporation in target cells in 3D microenvironments. *Cell.* 2020;9:1180. <https://doi.org/10.3390/cells9051180>.
38. Endisha H, Rockel J, Jurisica I, Kapoor M. The complex landscape of microRNAs in articular cartilage: biology, pathology, and therapeutic targets. *JCI Insight.* 2018;3:e121630. <https://doi.org/10.1172/jci.insight.121630>.
39. Dubin JA, Greenberg DR, Iglinski-Benjamin KC, Abrams GD. Effect of micro-RNA on tenocytes and tendon-related gene expression: a systematic review. *J Orthop Res.* 2018;36:2823-2829. <https://doi.org/10.1002/jor.24064>.
40. Thankam FG, Boosani CS, Dilisio MF, Agrawal DK. MicroRNAs associated with inflammation in shoulder tendinopathy and glenohumeral arthritis. *Mol Cell Biochem.* 2018;437:81-97. <https://doi.org/10.1007/s11010-017-3097-7>.
41. Li YS, Luo W, Zhu SA, Lei GH. T cells in osteoarthritis: alterations and beyond. *Front Immunol.* 2017;8:356. <https://doi.org/10.3389/fimmu.2017.00356>.
42. Tang C, Chen Y, Huang J, et al. The roles of inflammatory mediators and immunocytes in tendinopathy. *J Orthop Translat.* 2018;14:23-33. <https://doi.org/10.1016/j.jot.2018.03.003>.
43. Xu SJ, Hu HT, Li HL, et al. The role of miRNAs in immune cell development, immune cell activation, and tumor immunity: with a focus on macrophages and natural killer cells. *Cells.* 2019;8:1140. <https://doi.org/10.3390/cells8101140>.
44. Lorenzo P, Bayliss MT, Heinegård D. Altered patterns and synthesis of extracellular matrix macromolecules in early osteoarthritis. *Matrix Biol.* 2004;23:381-391. <https://doi.org/10.1016/j.matbio.2004.07.007>.
45. Riley GP. Gene expression and matrix turnover in overused and damaged tendons. *Scand J Med Sci Sports.* 2005;15:241-251. <https://doi.org/10.1111/j.1600-0838.2005.00456.x>.
46. Del Buono A, Oliva F, Osti L, et al. Metalloproteinases and tendinopathy. *Muscles Ligaments Tendons J.* 2013;3:51-57. <https://doi.org/10.11138/mltj/2013.3.1.051>.
47. Choi HR, Kondo S, Hirose K, Ishiguro N, Hasegawa Y, Iwata H. Expression and enzymatic activity of MMP-2 during healing process of the acute supraspinatus tendon tear in rabbits. *J Orthop Res.* 2002;20:927-933. [https://doi.org/10.1016/S0736-0266\(02\)00016-5](https://doi.org/10.1016/S0736-0266(02)00016-5).
48. Bedi A, Kovacevic D, Hettrich C, et al. The effect of matrix metalloproteinase inhibition on tendon-to-bone healing in a rotator cuff repair model. *J Shoulder Elbow Surg.* 2010;19:384-391. <https://doi.org/10.1016/j.jse.2009.07.010>.
49. Alfredson H. The chronic painful Achilles and patellar tendon: research on basic biology and treatment. *Scand J Med Sci Sports.* 2005;15:252-259. <https://doi.org/10.1111/j.1600-0838.2005.00466.x>.
50. Clements DN, Fitzpatrick N, Carter SD, Day PJR. Cartilage gene expression correlates with radiographic severity of canine elbow osteoarthritis. *Vet J.* 2009;179:211-218. <https://doi.org/10.1016/j.tvjl.2007.08.027>.
51. Alam MR, Ji JR, Kim MS, Kim NS. Biomarkers for identifying the early phases of osteoarthritis secondary to medial patellar luxation in dogs. *J Vet Sci.* 2011;12:273-280. <https://doi.org/10.4142/jvs.2011.12.3.273>.



52. Juneja SC. Cellular distribution and gene expression profile during flexor tendon graft repair: a novel tissue engineering approach. *J Tissue Eng.* 2013;4:2041731413492741. <https://doi.org/10.1177/2041731413492741>.
53. Freeberg MAT, Farhat YM, Easa A, et al. Serpine1 knockdown enhances MMP activity after flexor tendon injury in mice: implications for adhesions therapy. *Sci Rep.* 2018;8:5810. <https://doi.org/10.1038/s41598-018-24144-1>.
54. Li J, Ny A, Leonardsson G, Nandakumar KS, Holmdahl R, Ny T. The plasminogen activator/plasmin system is essential for development of the joint inflammatory phase of collagen type II-induced arthritis. *Am J Pathol.* 2005;166:783-792. [https://doi.org/10.1016/S0002-9440\(10\)62299-7](https://doi.org/10.1016/S0002-9440(10)62299-7).
55. Blanco Garcia FJ. Catabolic events in osteoarthritic cartilage. *Osteoarthr Cartil.* 1999;7:308-309. <https://doi.org/10.1053/joca.1998.0174>.
56. Xia W, de Bock C, Murrell GA, et al. Expression of urokinase-type plasminogen activator and its receptor is up-regulated during tendon healing. *J Orthop Res.* 2003;21:819-825. [https://doi.org/10.1016/S0736-0266\(03\)00058-5](https://doi.org/10.1016/S0736-0266(03)00058-5).
57. Dreier R, Wallace S, Fuchs S, Bruckner P, Grässel S. Paracrine interactions of chondrocytes and macrophages in cartilage degradation: articular chondrocytes provide factors that activate macrophage-derived pro-gelatinase B (pro-MMP-9). *J Cell Sci.* 2001;114:3813-3822.
58. Abrahamsson SO, Lohmander S. Differential effects of insulin-like growth factor-I on matrix and DNA synthesis in various regions and types of rabbit tendons. *J Orthop Res.* 1996;14:370-376. <https://doi.org/10.1002/jor.1100140305>.
59. Jenniskens YM, Koevoet W, de Bart AC, et al. Biochemical and functional modulation of the cartilage collagen network by IGF1, TGFbeta2 and FGF2. *Osteoarthritis Cartilage.* 2006;14:1136-1146. <https://doi.org/10.1016/j.joca.2006.04.002>.
60. Kelley KM, Oh Y, Gargosky SE, et al. Insulin-like growth factor-binding proteins (IGFBPs) and their regulatory dynamics. *Int J Biochem Cell Biol.* 1996;28:619-637. [https://doi.org/10.1016/1357-2725\(96\)00005-2](https://doi.org/10.1016/1357-2725(96)00005-2).
61. Dahlgren LA, Mohammed HO, Nixon AJ. Expression of insulin-like growth factor binding proteins in healing tendon lesions. *J Orthop Res.* 2006;24:183-192. <https://doi.org/10.1002/jor.20000>.
62. Dahlgren LA, Mohammed HO, Nixon AJ. Temporal expression of growth factors and matrix molecules in healing tendon lesions. *J Orthop Res.* 2005;23:84-92. <https://doi.org/10.1016/j.orthres.2004.05.007>.
63. Abate M, Guelfi M, Pantalone A, et al. Therapeutic use of hormones on tendinopathies: a narrative review. *Muscles Ligaments Tendons J.* 2016;6:445-452. <https://doi.org/10.11138/mltj/2016.6.4.445>.
64. McQuillan DJ, Handley CJ, Campbell MA, et al. Stimulation of proteoglycan biosynthesis by serum and insulin-like growth factor-I in cultured bovine articular cartilage. *Biochem J.* 1986;240:423-430. <https://doi.org/10.1042/bj2400423>.
65. Martin JA, Miller BA, Scherb MB, Lembke LA, Buckwalter JA. Co-localization of insulin-like growth factor binding protein 3 and fibronectin in human articular cartilage. *Osteoarthr Cartil.* 2002;10:556-563. <https://doi.org/10.1053/joca.2002.0791>.
66. Latourte A, Cherifi C, Maillet J, et al. Systemic inhibition of IL-6/Stat3 signalling protects against experimental osteoarthritis. *Ann Rheum Dis.* 2017;76:748-755. <https://doi.org/10.1136/annrheumdis-2016-209757>.
67. Ryu JH, Yang S, Shin Y, Rhee J, Chun CH, Chun JS. Interleukin-6 plays an essential role in hypoxia-inducible factor 2 $\alpha$ -induced experimental osteoarthritic cartilage destruction in mice. *Arthritis Rheum.* 2011;63:2732-2743. <https://doi.org/10.1002/art.30451>.
68. Morita W, Snelling SJ, Dakin SG, et al. Profibrotic mediators in tendon disease: a systematic review. *Arthritis Res Ther.* 2016;18:269. <https://doi.org/10.1186/s13075-016-1165-0>.
69. van Beuningen HM, Glansbeek HL, van der Kraan PM, van den Berg WB. Osteoarthritis-like changes in the murine knee joint resulting from intra-articular transforming growth factor-beta injections. *Osteoarthr Cartil.* 2000;8:25-33. <https://doi.org/10.1053/joca.1999.0267>.
70. Kehl D, Generali M, Mallone A, et al. Proteomic analysis of human mesenchymal stromal cell secretomes: a systematic comparison of the angiogenic potential. *NPJ Regen Med.* 2019;4(8):8. <https://doi.org/10.1038/s41536-019-0070-y>.
71. Ragni E, Perucca Orfei C, De Luca P, et al. Inflammatory priming enhances mesenchymal stromal cell secretome potential as a clinical product for regenerative medicine approaches through secreted factors and EV-miRNAs: the example of joint disease. *Stem Cell Res Ther.* 2020;11:165. <https://doi.org/10.1186/s13287-020-01677-9>.
72. Le Y, Zhou Y, Iribarren P, et al. Chemokines and chemokine receptors: their manifold roles in homeostasis and disease. *Cell Mol Immunol.* 2004;1:95-104.
73. Palomino DC, Marti LC. Chemokines and immunity. *Einstein.* 2015;13:469-473. <https://doi.org/10.1590/S1679-45082015RB3438>.
74. de Lange-Brokaar BJ, Ioan-Facsinay A, van Osch GJ, et al. Synovial inflammation, immune cells and their cytokines in osteoarthritis: a review. *Osteoarthr Cartil.* 2012;20:1484-1499. <https://doi.org/10.1016/j.joca.2012.08.027>.
75. Sharma P, Maffulli N. Biology of tendon injury: healing, modeling and remodeling. *J Musculoskelet Neuronal Interact.* 2006;6:181-190.
76. Hamilton JA. Colony-stimulating factors in inflammation and autoimmunity. *Nat Rev Immunol.* 2008;8:533-544. <https://doi.org/10.1038/nri2356>.
77. Haynes MK, Hume EL, Smith JB. Phenotypic characterization of inflammatory cells from osteoarthritic synovium and synovial fluids. *Clin Immunol.* 2002;105:315-325. <https://doi.org/10.1006/clim.2002.5283>.
78. Ishii H, Tanaka H, Katoh K, Nakamura H, Nagashima M, Yoshino S. Characterization of infiltrating T cells and Th1/Th2-type cytokines in the synovium of patients with osteoarthritis. *Osteoarthr Cartil.* 2002;10:277-281. <https://doi.org/10.1053/joca.2001.0509>.
79. Jomaa G, Kwan CK, Fu SC, et al. A systematic review of inflammatory cells and markers in human tendinopathy. *BMC Musculoskelet Disord.* 2020;21:78. <https://doi.org/10.1186/s12891-020-3094-y>.
80. Yang L, Boldin MP, Yu Y, et al. miR-146a controls the resolution of T cell responses in mice. *J Exp Med.* 2012;209:1655-1670. <https://doi.org/10.1084/jem.20112218>.
81. Rossi RL, Rossetti G, Wenandy L, et al. Distinct microRNA signatures in human lymphocyte subsets and enforcement of the naive state in CD4+ T cells by the microRNA miR-125b. *Nat Immunol.* 2011;12:796-803. <https://doi.org/10.1038/ni.2057>.
82. Fayyad-Kazan H, Hamade E, Rouas R, et al. Downregulation of microRNA-24 and -181 parallels the upregulation of IFN- $\gamma$  secreted by activated human CD4 lymphocytes. *Hum Immunol.* 2014;75:677-685. <https://doi.org/10.1016/j.humimm.2014.01.007>.
83. Sang W, Zhang C, Zhang D, et al. MicroRNA-181a, a potential diagnosis marker, alleviates acute graft versus host disease by regulating IFN- $\gamma$  production. *Am J Hematol.* 2015;90:998-1007. <https://doi.org/10.1002/ajh.24136>.
84. Steiner DF, Thomas MF, Hu JK, et al. MicroRNA-29 regulates T-box transcription factors and interferon- $\gamma$  production in helper T cells. *Immunity.* 2011;35:169-181. <https://doi.org/10.1016/j.immuni.2011.07.009>.
85. Li S, Wan J, Anderson W, et al. Downregulation of IL-10 secretion by Treg cells in osteoarthritis is associated with a reduction in Tim-3 expression. *Biomed Pharmacother.* 2016;79:159-165. <https://doi.org/10.1016/j.biopha.2016.01.036>.
86. Salles JI, Lopes LR, Duarte MEL, et al. Fc receptor-like 3 (-169T>C) polymorphism increases the risk of tendinopathy in volleyball

- athletes: a case control study. *BMC Med Genet.* 2018;19:119. <https://doi.org/10.1186/s12881-018-0633-6>.
87. Lu LF, Boldin MP, Chaudhry A, et al. Function of miR-146a in controlling Treg cell-mediated regulation of Th1 responses. *Cell.* 2010;142:914-929. <https://doi.org/10.1016/j.cell.2010.08.012>.
  88. Warth SC, Hoefig KP, Hiekel A, et al. Induced miR-99a expression represses Mtor cooperatively with miR-150 to promote regulatory T-cell differentiation. *EMBO J.* 2015;34:1195-1213. <https://doi.org/10.15252/embj.201489589>.
  89. Gao Y, Lin F, Su J, et al. Molecular mechanisms underlying the regulation and functional plasticity of FOXP3(+) regulatory T cells. *Genes Immun.* 2012;13:1-13. <https://doi.org/10.1038/gene.2011.77>.
  90. Self-Fordham JB, Naqvi AR, Uttamani JR, Kulkarni V, Nares S. MicroRNA: dynamic regulators of macrophage polarization and plasticity. *Front Immunol.* 2017;8:1062. <https://doi.org/10.3389/fimmu.2017.01062>.
  91. Fordham JB, Naqvi AR, Nares S. Regulation of miR-24, miR-30b, and miR-142-3p during macrophage and dendritic cell differentiation potentiates innate immunity. *J Leukoc Biol.* 2015;98:195-207. <https://doi.org/10.1189/jlb.1A1014-519RR>.
  92. Niu X, Schulert GS. Functional regulation of macrophage phenotypes by MicroRNAs in inflammatory arthritis. *Front Immunol.* 2019;10:2217. <https://doi.org/10.3389/fimmu.2019.02217>.
  93. Ying X, Wu Q, Wu X, et al. Epithelial ovarian cancer-secreted exosomal miR-222-3p induces polarization of tumor-associated macrophages. *Oncotarget.* 2016;7:43076-43087. <https://doi.org/10.18632/oncotarget.9246>.
  94. Zavatti M, Beretti F, Casciaro F, Bertucci E, Maraldi T. Comparison of the therapeutic effect of amniotic fluid stem cells and their exosomes on monoiodoacetate-induced animal model of osteoarthritis. *Biofactors.* 2020;46:106-117. <https://doi.org/10.1002/biof.1576>.
  95. Li X, Gibson G, Kim JS, et al. MicroRNA-146a is linked to pain-related pathophysiology of osteoarthritis. *Gene.* 2011;480:34-41. <https://doi.org/10.1016/j.gene.2011.03.003>.
  96. Kopańska M, Szala D, Czech J, et al. MiRNA expression in the cartilage of patients with osteoarthritis. *J Orthop Surg Res.* 2017;12:51. <https://doi.org/10.1186/s13018-017-0542-y>.
  97. Jia D, Li Y, Han R, et al. miR-146a-5p expression is upregulated by the CXCR4 antagonist TN14003 and attenuates SDF-1-induced cartilage degradation. *Mol Med Rep.* 2019;19:4388-4400. <https://doi.org/10.3892/mmr.2019.10076>.
  98. Philipot D, Guérit D, Platano D, et al. p16INK4a and its regulator miR-24 link senescence and chondrocyte terminal differentiation-associated matrix remodeling in osteoarthritis. *Arthritis Res Ther.* 2014;16:R58. <https://doi.org/10.1186/ar4494>.
  99. Wu YH, Liu W, Zhang L, et al. Effects of microRNA-24 targeting C-myc on apoptosis, proliferation, and cytokine expressions in chondrocytes of rats with osteoarthritis via MAPK signaling pathway. *J Cell Biochem.* 2018;119:7944-7958. <https://doi.org/10.1002/jcb.26514>.
  100. Munro TM, Thankam FG, Dilisio MF, Gross RM, Boosani CS, Agrawal DK. Disease-specific microRNAs regulating extracellular matrix and matrix metalloproteinases in tendinopathy. *Curr Mol Biol Rep.* 2018;4:198-207. <https://doi.org/10.1007/s40610-018-0103-0>.
  101. Magatti M, Masserdotti A, Bonassi Signoroni P, et al. B lymphocytes as targets of the immunomodulatory properties of human amniotic mesenchymal stromal cells. *Front Immunol.* 2020;11:1156. <https://doi.org/10.3389/fimmu.2020.01156>.
  102. Cargnoni A, Gibelli L, Tosini A, et al. Transplantation of allogeneic and xenogeneic placenta-derived cells reduces bleomycin-induced lung fibrosis. *Cell Transplant.* 2009;18:405-422. <https://doi.org/10.3727/096368909788809857>.
  103. Cargnoni A, Ressel L, Rossi D, et al. Conditioned medium from amniotic mesenchymal tissue cells reduces progression of bleomycin-induced lung fibrosis. *Cytotherapy.* 2012;14:153-161. <https://doi.org/10.3109/14653249.2011.613930>.
  104. Cargnoni A, Piccinelli EC, Ressel L, et al. Conditioned medium from amniotic membrane-derived cells prevents lung fibrosis and preserves blood gas exchanges in bleomycin-injured mice-specificity of the effects and insights into possible mechanisms. *Cytotherapy.* 2014;16:17-32. <https://doi.org/10.1016/j.jcyt.2013.07.002>.
  105. Carbone A, Castellani S, Favia M, et al. Correction of defective CFTR/ENaC function and tightness of cystic fibrosis airway epithelium by amniotic mesenchymal stromal (stem) cells. *J Cell Mol Med.* 2014;18:1631-1643. <https://doi.org/10.1111/jcmm.12303>.
  106. Cargnoni A, Romele P, Bonassi Signoroni P, et al. Amniotic MSCs reduce pulmonary fibrosis by hampering lung B-cell recruitment, retention, and maturation. *STEM CELLS TRANSLATIONAL MEDICINE.* 2020;9:1023-1035. <https://doi.org/10.1002/sctm.20-0068>.
  107. Lee PH, Tu CT, Hsiao CC, et al. Antifibrotic activity of human placental amnion membrane-derived CD34+ mesenchymal stem/progenitor cell transplantation in mice with thioacetamide-induced liver injury. *STEM CELLS TRANSLATIONAL MEDICINE.* 2016;5:1473-1484. <https://doi.org/10.5966/sctm.2015-0343>.
  108. Tuca AC, Ertl J, Hingerl K, et al. Comparison of Matrigel and Matrigel as a carrier for human amnion-derived mesenchymal stem cells in wound healing. *Placenta.* 2016;48:99-103. <https://doi.org/10.1016/j.placenta.2016.10.015>.
  109. Kim SW, Zhang HZ, Guo L, Kim JM, Kim MH. Amniotic mesenchymal stem cells enhance wound healing in diabetic NOD/SCID mice through high angiogenic and engraftment capabilities. *PLoS One.* 2012;7:e41105. <https://doi.org/10.1371/journal.pone.0041105>.
  110. Parolini O, Souza-Moreira L, O'Valle F, et al. Therapeutic effect of human amniotic membrane-derived cells on experimental arthritis and other inflammatory disorders. *Arthritis Rheumatol.* 2014;66:327-339. <https://doi.org/10.1002/art.38206>.
  111. Onishi R, Ohnishi S, Higashi R, et al. Human amnion-derived mesenchymal stem cell transplantation ameliorates dextran sulfate sodium-induced severe colitis in rats. *Cell Transplant.* 2015;24:2601-2614. <https://doi.org/10.3727/096368915X687570>.
  112. Pischiutta F, Brunelli L, Romele P, et al. Protection of brain injury by amniotic mesenchymal stromal cell-secreted metabolites. *Crit Care Med.* 2016;44:e1118-e1131. <https://doi.org/10.1097/CCM.0000000000001864>.
  113. Shu J, Pan L, Huang X, et al. Transplantation of human amnion mesenchymal cells attenuates the disease development in rats with collagen-induced arthritis. *Clin Exp Rheumatol.* 2015;33:484-490.
  114. De Luca P, Kouroupis D, Viganò M, et al. Human diseased articular cartilage contains a mesenchymal stem cell-like population of chondroprogenitors with strong immunomodulatory responses. *J Clin Med.* 2019;8:423. <https://doi.org/10.3390/jcm8040423>.
  115. Viganò M, Lugano G, Perucca Orfei C, et al. Autologous micro-fragmented adipose tissue reduces inflammatory and catabolic markers in supraspinatus tendon cells derived from patients affected by rotator cuff tears. *Int Orthop.* 2020;45:419-426. <https://doi.org/10.1007/s00264-020-04693-9>.
  116. Murphy G, Lee MH. What are the roles of metalloproteinases in cartilage and bone damage? *Ann Rheum Dis.* 2005;64:iv44-iv47. <https://doi.org/10.1136/ard.2005.042465>.
  117. Wuchter P, Bieback K, Schrezenmeier H, et al. Standardization of good manufacturing practice-compliant production of bone marrow-derived human mesenchymal stromal cells for immunotherapeutic applications. *Cytotherapy.* 2015;17:128-139. <https://doi.org/10.1016/j.jcyt.2014.04.002>.



118. de Wolf C, van de Bovenkamp M, Hoefnagel M. Regulatory perspective on in vitro potency assays for human mesenchymal stromal cells used in immunotherapy. *Cytotherapy*. 2017;19:784-797. <https://doi.org/10.1016/j.jcyt.2017.03.076>

#### SUPPORTING INFORMATION

Additional supporting information may be found online in the Supporting Information section at the end of this article.

**How to cite this article:** Ragni E, Papait A, Perucca Orfei C, et al. Amniotic membrane-mesenchymal stromal cells secreted factors and extracellular vesicle-miRNAs: Anti-inflammatory and regenerative features for musculoskeletal tissues. *STEM CELLS Transl Med*. 2021;10:1044-1062. <https://doi.org/10.1002/sctm.20-0390>